Faculty of Graduate Studies Chemistry Department

Development of Prolonged Release Oil-Core Polymeric Nanocapsule Encapsulating Copper Diethyldithiocarbamate for Treating Lung Cancer

By:

Rasheedah Farhat Abu-Hamdia

Supervisor:

Dr. Mosab Abu Reesh

Co-supervisor:

Dr. Mohammed Qaisiya

This Thesis Submitted in Partial Fulfillment of the Requirements for the Degree of Master of Chemistry, College of Graduate Studies & Academic Research, Hebron University, Palestine.

2022

Committee Decision

We, the undersigned, approve the Master's Thesis of Rasheedah Abu-Hamdia.

Thesis Title: Development of Prolonged Release Oil-Core Polymeric Nanocapsule Encapsulating Copper Diethyldithiocarbamate for Treating Lung Cancer.

This thesis was successfully defended on June, 2022 and approved by:

Committee members		Signature
Supervisor	Dr. Mosab Abu Alreesh	----------
Co-supervisor	Dr. Mohammed Qaisiya	----------
Internal examiner	Dr. Sami Makharza	----------
External examiner	Dr. Derar Smadi	----------

Dedication

I wouldn't have been able to go any step further without my family, my parents, sweet sisters, and brothers who were all supporting me every time.

I also dedicate this work to Dr. Omar Abu Abed, for his support, assistance, and effort in finishing my thesis.

Also, I would be happy to say thank you to my dearest colleagues who didn't hesitate to offer help when I needed it, Majdoleen Atawnah. and can't forget who made my years lighter in university Sahar and Razan.

I would like to say that I am grateful to my supervisor, Dr. Mosab Abu Reesh for his invaluable advice, continuous support and patients during my master's study.

Acknowledgement

There is no acknowledgment that can express my gratitude, appreciation, and thanks for the tremendous amount of support, assistance and guidance during this journey that I received from Dr. Omar Abu Abed. Also, I would like to extend my sincere thanks to my supervisor Dr. Dr. Mosab Abu Reesh.

I would like to express my gratitude and thanks for the support given by the faculty members of the chemistry department at Hebron University. I also would like to appreciate the help provided by the lab teachers at the faculty of pharmacy and medical science.

Table of contents

List of Tables

List of Figures

List of Abbreviations

ADH	*Alcohol Dehydrogenase*
ALDH	*Aldehyde Dehydrogenase*
ANG	*Angiogenin*
ANOVA	*One-Way Analysis of Variance*
Cc	*Characteristic Curvature*
CCO	*Cytochrome C Oxidase*
CuAO	*Copper Containing Amine Oxidase*
$Cu(DDC)_2$	*Bis (N, N-diethyldithiocarbamate) Cu (II)*
C.N	*Coordination Number*
C.P	*Ceruloplasmin*
DAO	*Diamine Oxidase*
DDC	*Diethyldithiocarbamate*
DMSO	*Dimethyl Sulfoxide*
DSF	*Disulfiram*
DβM	*Dopamine β-Monooxygenase*
EE	*Encapsulation Efficiency*
EPR	*Enhanced Permeability and Retention*
ERK	*Extracellular Signal-Regulated Kinas*
FBS	*Fetal Bovine Serum*
FDA	*Food and Drug Administration*
FD	*Free Drug*
FT-IR	*Fourier-Transform Infrared Spectroscopy*
HLB	*Hydrophilic-Lipophilic Balance*
HMPB	*Hollow Mesoporous Prussian Blue*
JNK	*c-Jun N-terminal Kinas*
LOX	*Lysyl Oxidase*
MAPK	*Mitogen-Activated Protein Kinas*
Me-DDC	*S-methyl-diethyldithiocarbamate*
Me-DDC sulfoxide	*S-methyl-diethyldithiocarbamate sulfoxide*
Me-DTC sulfoxide	*S-methyl-diethylthiocarbamate sulfoxide*
NC	*Nanocapsules*
NF-kB	*Nuclear Factor Kappa B*
N.P	*Nanoparticle*
o/w emulsion	*Oil-in-Water Emulsion*
PBS	*Phosphate Buffer Saline*
PCL	*Polycaprolactone*
PDI	*Polydispersity Index*

PEG	*Polyethylene glycol*
PLGA	*Poly (lactic-co-glycolic acid)*
PTX	*Paclitaxel*
p-value	*Two-Tailed Significance*
RHLB	*Required HLB*
ROS	*Reactive Oxygen Species*
SD	*Standard Deviation*
SLNs	*Solid Lipid Nanoparticles*
SOD1	*Superoxide Dismutase*
UPS	*Ubiquitin-Proteasome System*
UV-vis	*Ultra Violet-Visible Spectroscopy*
w/o emulsion	*Water-in-Oil Emulsion*
Z-Average diameter	*Hydrodynamic Size*
%EE	*Percentages Encapsulation Efficiency*
%LE	*Percentage Protein Loading*

Abstract

Drug repurposing has become an attractive way to treat diseases; it involves the use of compounds with no hazard. Disulfiram (DSF), a well-known drug for the treatment of alcoholism with the approvement of the Food and Drug Administration (FDA) since 1951, has been found to have an anti-cancer effect when chelation with copper (II) ions forming bis (N, N-diethyldithiocarbamate) Cu (II) complex ($Cu(DDC)_2$). The main limitations of $Cu(DDC)_2$ complex are its poor solubility in aqueous media and compromised stability in serum. In this study, nanotechnology has been facilitated to enhance the delivery of this complex to cancer cells by emulsification. Polyethylene glycol (PEG) and polycaprolactone (PCL) have been used to enhance the stability, biocompatibility, and reduce the hydrophobicity of the nanoemulsion, gaining a longer circulation lifetime in the body; increasing the efficiency of the therapy. PEG and PCL have been used in three different ratios including 25:75, 50:50, and 75:25, to detect the most suitable nanoparticle (N.P) properties for the delivery of the drug. $Cu(DDC)_2$ as a free drug has been characterized using FT-IR, UV-vis techniques. The encapsulation efficiency, particle size, zeta potential, drug release, serum stability, and cytotoxicity of the prepared nanoparticles have been studied.

Chapter One:

Introduction

1.1. Cancer

Healthy cells grow and divide with a specific life cycle. Cancer disrupts this cycle leading to abnormal cell growth caused by changes or mutation in DNA [1]. DNA is the leader that instructs the cells how to perform, grow, and divide; therefore, any uncorrected mutations may turn into cancerous cells. Mutant cells can grow and divide uncontrollably, causing tumours [2], [3]. Depending on where these tumours grow, a large group of diseases arises (about 200) [4].

Tumours can be divided into two major types; benign and malignant. Benign tumours are noncancerous and do not spread to other tissues and organs. While malignancy is a cancerous tumour that keeps growing, spreading, and can travel throughout the body to form new tumours by metastasis [1].

Cancer is one of the most potentially life-threatening diseases [5]. It may exist anywhere in the body. Cancer mechanisms were ambiguous and mysterious until oncologists understood cancers in the last century. They have achieved noteworthy advances in cancer diagnosis, prevention, and treatment. A wide range of treatments is possible. The most common treatment strategy used includes surgery, radiation therapy, and chemotherapy. Some general complications accompany cancer treatment protocols, e.g., fatigue, nausea, loss of appetite, anaemia, hair loss, pain, lymphedema, insomnia, and immune system depression. Cancer researchers are ongoing to identify newer treatments. A treatment that is more specific and selective toward cancer cells rather than normal cells is a crucial need to enhance safety. Lead to more effective treatment with lower toxicity to other tissues. These objectives and goals can be achieved by targeted drug therapy [3].

1.2. Drug Delivery and Nanotechnology

Drug delivery systems are engineered technologies that improve drug performance efficiency by three different strategies. These strategies include but are not limited to; targeted delivery, solubility enhancement, and controlled release. Targeted delivery can enhance the drug efficiency and minimize toxicity and drug side effect, as the drug is directed to specific tissues, organs, or even cells, with minimal access to healthy cells. Solubility enhancement increases circulation time in the body for lipophilic and hydrophobic drugs and prevents aggregation to improve their pharmacokinetic properties. Controlling drug release enables the maintenance of the effective dose of drugs in the body, increasing drug efficiency [6,7].

Nanotechnology is curbing new roads for drug delivery carriers. It is material engineering within a size range of less than 1 micrometre [8,9]. Utilising nanotechnology as a strategy to innovate drug delivery systems can protect drugs from degradation, improve the bioavailability as circulation time increase and biocompatibility of drugs, and enhance cell penetration efficiency; hence, increasing targeted delivery, solubility enhancement, and controlled release of the drug [7].

To prepare successful drug delivery nanoparticles, three main properties must be considered to overcome delivery barriers: size, shape, and surface charge [10]. Nanoparticle with an average size around 100 nm has shown the best circulation time, where particles with size less than 5 nm directly undergo renal clearance, and 200-500 nm particles face splenic filtration [10]. For the shape, filomicelles shape shows longer circulation time, higher drug loading, and drug release [11,12]. Discoidal particles have the largest adhesion to vessel walls due to the large surface area, where the spherical shape beats discoidal particles in cellular uptake since the uptake of spherical particles was the fastest [10,12]. Finally, neutral and slightly negative nanoparticles

have shown a longer circulation time than positive ones. On the other hand, positively charged nanoparticles have a higher uptake rate in most cell types [13,14].

Nanoparticles can be divided into organic, i.e., polymeric, lipid-based, and carbon-based nanomaterials, inorganic consisting of metals and semi-metals, or hybrid systems of two or more types of N.P.s. Polymeric N.P.s, with their wide range offering numerous modifications with a small possibility for aggregation and toxicity. Lipid-based N.P.s have the best bioavailability but a low encapsulation efficiency. Carbon-based N.P.s with a relatively high surface area and easy surface modification. The inorganic N.P.s have superior and unique magnetic, electrical, and optical properties, but their low solubility and toxicity are known [15-17].

According to the nanoparticle type used, nanoparticles can offer different ways to deliver drugs, where the drug can be coupled or complexed with the drug carrier, adsorbed on the surface, embedded, or encapsulated in the core. Lipid-based, carbon-based, and polymeric nanoparticles can offer all types. The easiest way for inorganic nanoparticles is surface adsorption or complexation [18,19].

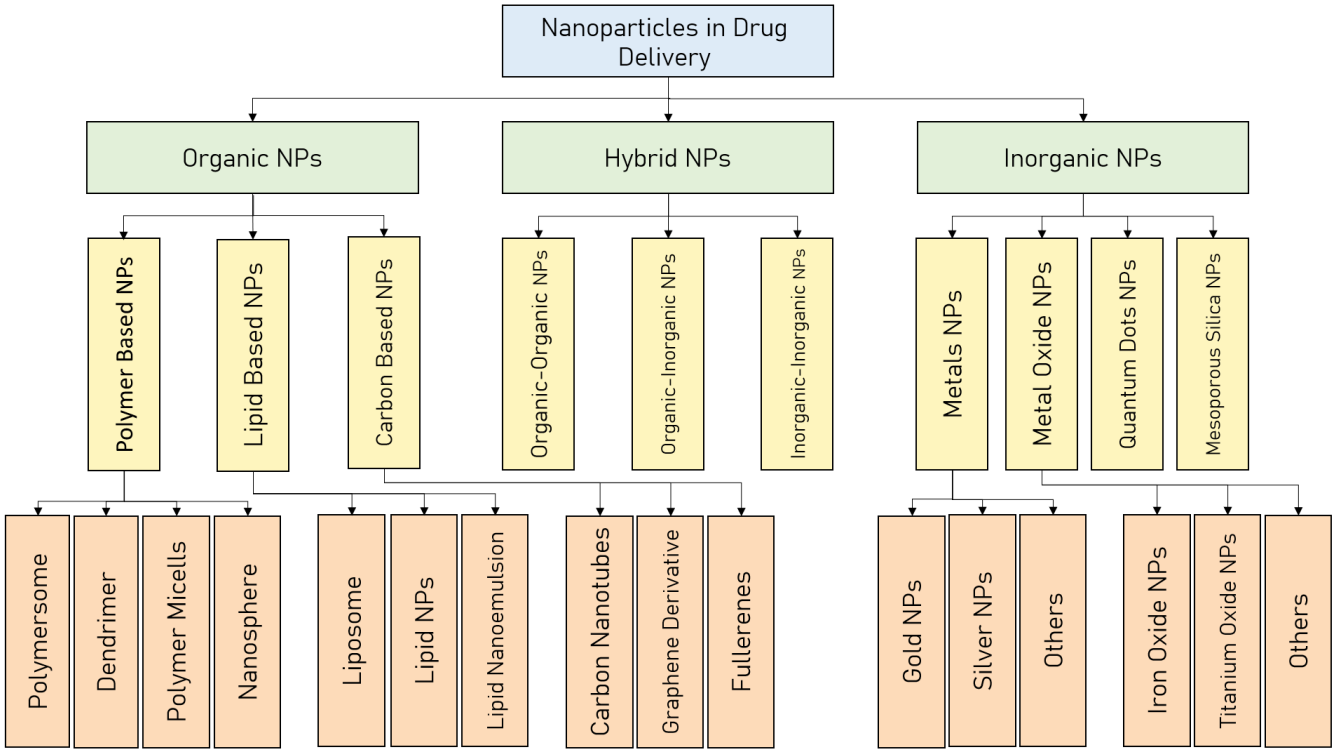

***Figure 1**. Classification of nanoparticles used for therapeutical application and drug delivery.*

1.3. Emulsification

"Like dissolves like", a well-known rule that describes the relationship between polar (hydrophilic) and non-polar (lipophilic) solvent and solute. Where polar solvents dissolve hydrophilic solutes, while non-polar solvents dissolve non-polar solutes. However, hydrophilic and lipophilic solvents and solutes can really be mixed together with the right ingredients. An essential ingredient for this dissolvation is known as emulsifiers [20]. Emulsifiers are a class of surfactants that are used as emulsion stabilisers [21]. It consists of a hydrophilic head and lipophilic tail, lowering the interfacial tension between aqueous and organic phases [22] , and providing a physical barrier between the droplets of solute preventing accumulation and eases the formation of an emulsion. If the emulsifier dispersed the organic (oil) droplets in an aqueous phase (water), it forms an oil-in-water (o/w) emulsion. Where the dispersion of aqueous droplets

in an organic phase forms water-in-oil (w/o) emulsion. Using emulsion as a drug delivery system has offered several advantages including enhancement of drug bioavailability, drug stability, and prolonged drug action [22].

Selecting the right emulsifier to gain the most stable emulsion is an important step. To facilitate the selection step, one can refer to hydrophilic-lipophilic balance (HLB). The HLB is a scale range from 0 to 20. Where 0 -10 values represent the lipophilic surfactants and emulsifiers, and 10 - 20 values represent the hydrophilic ones. The emulsifiers with an HLB range from 3.5 to 6 favour the w/o emulsion, where the HLB values of 8 to 18 favour the o/w emulsion [23]. For the emulsification process, one or more emulsifiers can be used with an average HLB value. HLB value importance is not only for emulsifiers; where some oil phases have different HLB requirements (RHLB). For example, to prepare an o/w emulsion using castor oil, the RHLB value needed is 8 [22]. Another variable that can be used to choose the emulsifier is the Characteristic Curvature value (Cc). A negative Cc value represents hydrophilic emulsifiers that tend to produce o/w emulsion, while a positive Cc value represents lipophilic emulsifiers that tend to produce w/o emulsion [24,25].

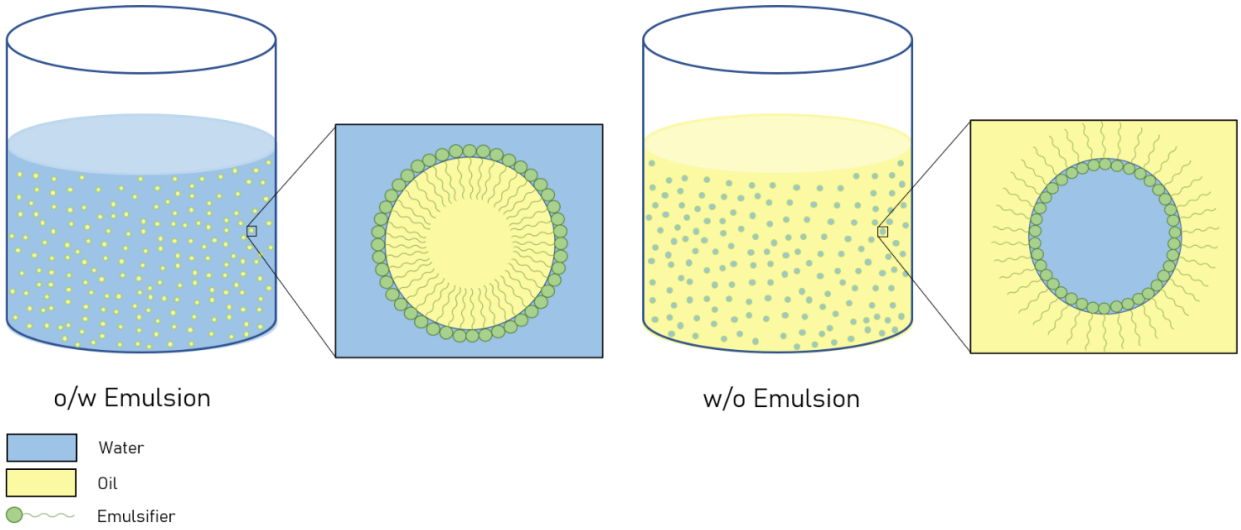

Figure 2. *O/w emulsion, w/o emulsion, and the difference between the emulsifier orientation, wherein the o/w emulsion the lipophilic tail is oriented inside to the oil droplet, and the hydrophilic head is oriented to the aqueous phase. In w/o emulsion the hydrophilic head is oriented inside to the water droplet, while the lipophilic tail is oriented to the organic phase.*

1.4. Disulfiram

Disulfiram (Bis(diethylthiocarbamoyl) disulfide – $C_{10}H_{20}N_2S_4$), is a white odourless powder, with a solubility in water reaches 20mg/100ml [26], highly unstable in acidic media [26], and rapidly metabolized in vivo (half-life = 4min) [27,28]. Commercially known as Antabuse®, Disulfiram is the drug of choice for the treatment of alcoholism since approved by Food and Drug Administration (FDA) in 1951[29-31].

The development of Disulfiram has been going through several stages since its effect was observed in the presence of alcohol and that was through various situations since 1930. The illness symptoms were noticed in people who exposed to or took a dose of Disulfiram and drank alcohol at the same time [30]. These observations motivated researchers to investigate the

effectiveness of Disulfiram clinically. Accordingly, the mechanism of disulfiram action was revealed.

Normally, alcohol can be metabolised by alcohol dehydrogenase (ADH) in the human body producing acetaldehyde. This metabolism may lead to another stage of metabolism by aldehyde dehydrogenase (ALDH) leading to acetic acid as a final product, which is a product that the human body has the ability to handle [32,33]. Consumption of alcohol in the presence of Disulfiram causes the consumer to feel unpleasant symptoms [34,35]. Then one may consume less to reduce these symptoms. Many studies were conducted to investigate the effect of Disulfiram (DSF) on the ALDH enzyme. It was found that Disulfiram blocks the activity of the ALDH enzyme [30,36], which is responsible for detoxing acetaldehyde by oxidising it and converting it to acetic acid. blocking this enzyme leads to the accumulation of acetaldehyde on the human body causing alcohol sensitivity [37].

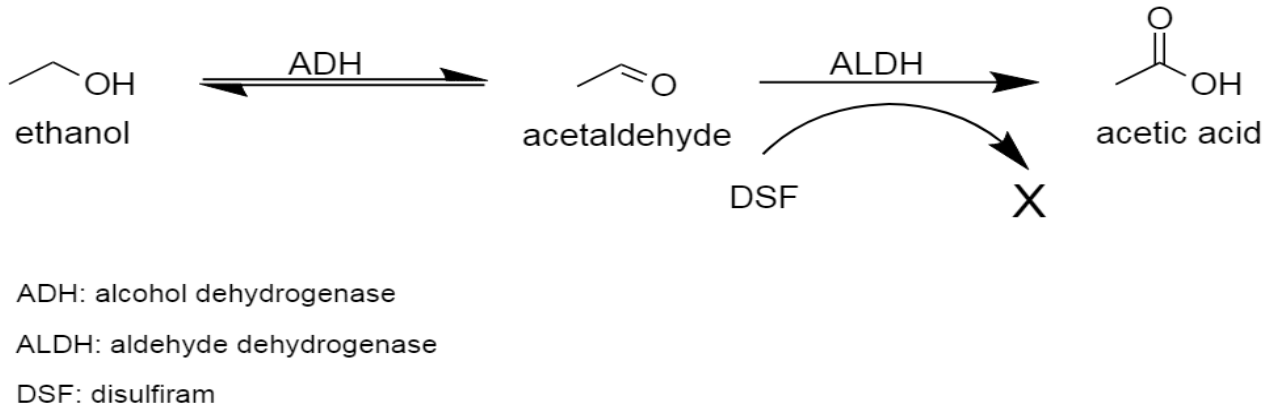

Figure 3. *Mechanism of alcohol metabolism and disulfiram effect. Normally, alcohol is oxidised into two steps to form acetic acid; the later can be excreted easily from the body. DSF increases the acetaldehyde which causes unpleasant symptoms inside the body.*

1.4.1. Traditional Disulfiram Formulations

Disulfiram is marketed under the name Antabuse. It is supplied as 200 - 500 mg round white tablets. These tablets can be taken orally as a tablet or ground and mixed with water or other drinks. Antabus average maintenance dosage is 250 mg/day(125-500 mg/day), with a maximum dosage of 500 mg/day [38]. The human body can absorb up to 80-95% of indented Disulfiram. The first dose of Antabuse can be taken after at least 12 h of alcohol consumption; to avoid Disulfiram - alcohol reaction, which can last up to two weeks after the last Antabuse dose[30].

As the Disulfiram - alcohol reaction can start after a few minutes of alcohol consumption, the elevated levels of acetaldehyde can be detected in the blood, causing an unpleasant effect. These effects can range from moderate to severe, moreover, it may last for a few hours, depending on the blood alcohol concentration. These symptoms include weakness, hypotension, tachycardia, sweating, hyperventilation or dyspnoea, headache, nausea and vomiting, and others [30,37].

Although Antabuse was the most common medication for alcoholism at the end of 20 century, after the recognition that Disulfiram have no effect on the elimination of alcohol from the body [30], it is now used as a support treatment for alcohol dependency, it is most likely used with patients who are motivated to quit alcohol in the initial stages.

1.5. Drug Repurposing

Recently, one of the strategies in anticancer drug development is drug repurposing. Through this method we can overcome many drugs development stages, including cytotoxicity study, side effect, drug resistance, and acquired chemoresistance. Repurposing a known drug with a

complete profile, a time saving promising strategy with lower coast, minimal risk, and elevated safety, compared with discovering and developing a new drug [39-42].

DSF has proved its effectiveness as an anticancer through different mechanisms [36], hence, repurposing of DSF as an anticancer drug is very promising.

1.5.1. Repurposing of Disulfiram Using

Disulfiram initially was known by its anti-alcohol activity. after many research that has been done about its effectiveness and behaviour in cells, it was found that Disulfiram and its metabolite diethyldithiocarbamate (DDC) have many activities. They act as antiviral, antibacterial, antifungal, and antiparasitic [43]. Moreover, they have the potential to treat cancer, by inhibiting proliferation and inducing cell death [44]. Afterwards, Disulfiram promising anticancer activity was intensively investigated on a wide range of cancer cell lines, which showed a remarkable efficiency [45]. The main cancer types that were eradicated by disulfiram and its derivatives are melanoma (skin) [44,46], breast [47,48], glioblastoma (brain) [49], prostate [50,51], lung [52-54], colorectal [55], and pancreatic cancer [56,57].

In addition to DSF's ability to inhibit ALDH, other actions were found, including the generation of Reactive Oxygen Species (ROS). Disturbing, the redox reaction balance in cells, which may lead to substantial damages in DNA, protein, and other cellular component [44].

Activation of mitogen-activated protein kinas (MAPK) pathway, which is a family of enzyme have control over many cellular processes including growth, differentiation, and stress response, hence, they are related with cancer cell progress, growth, and apoptosis [58]. MAPK family consists of the extracellular signal-regulated kinas (ERK), c-Jun n-terminal kinas (JNK), and

p38 MAPK. ERK pathway, which has the role of regulating cell growth, differentiation, and proliferation.

The JNK pathway is related to cell death or alteration of cellular proliferation and gene expression [59]. p38 MAPK pathway, which makes two opposite effects, enhancing cell growth, and apoptotic cell death [60,61], depending on cell and stimulation type [62]. Reported effect of DSF on MAPK include activation of ROS-JNK [63], and ROS-p38 MAPK that induce apoptosis [64].

DSF also inhibit nuclear factor kappa B (NF-kB) [65], and Nrf2 [63]. Furthermore, DSF inhibits the activity of the ubiquitin-proteasome system (UPS), a group of enzyme that plays an essential role in protein homeostasis maintenance, by the degradation of damaged or unneeded proteins, so, inhibition of UPS cause oxidative stress [66]. DSF also has the ability to inhibit angiogenesis [67], reverse drug resistance through different mechanisms [68], and enhance the sensitivity of cancer cells to radiotherapy (radio-sensitiser) [69,70].

The main obstacle that limits clinical applications of Disulfiram as an anticancer agent is its rapid metabolism in blood circulation. The half-life of DSF is 4 min, therefore, after these 4 min, only DSF metabolite can be detected in the body [28,71]. DSF metabolite includes diethyldithiocarbamate (DDC), which is also unstable and rapidly degraded to diethylamine and carbon disulfide, or form S-methyl-diethyldithiocarbamate (Me-DDC) or glucuronidated-DDC [37,[54]. Many hypothesis were suggested to explain the exact mechanism of DSF metabolism, and all of them agree that DSF can be converted into DDC or one of its derevatives immediately in the blood [44,72]. Frazier, K. R. et al 2019, suggested that DSF is converted into DDC. DDC is further metabolised to diethylamine and carbon disulfide, or methylated to form Me-DDC.

Me-DDC is further oxidised forming two final products, which are S-methyl-diethyldithiocarbamate sulfoxide (Me-DDC sulfoxide), and S-methyl-diethylthiocarbamate sulfoxide (Me-DTC sulfoxide) [73]. The sulfoxide metabolites, Me-DTC, and Me-DDC are the main inhibitors for ALDH[37,72,73].

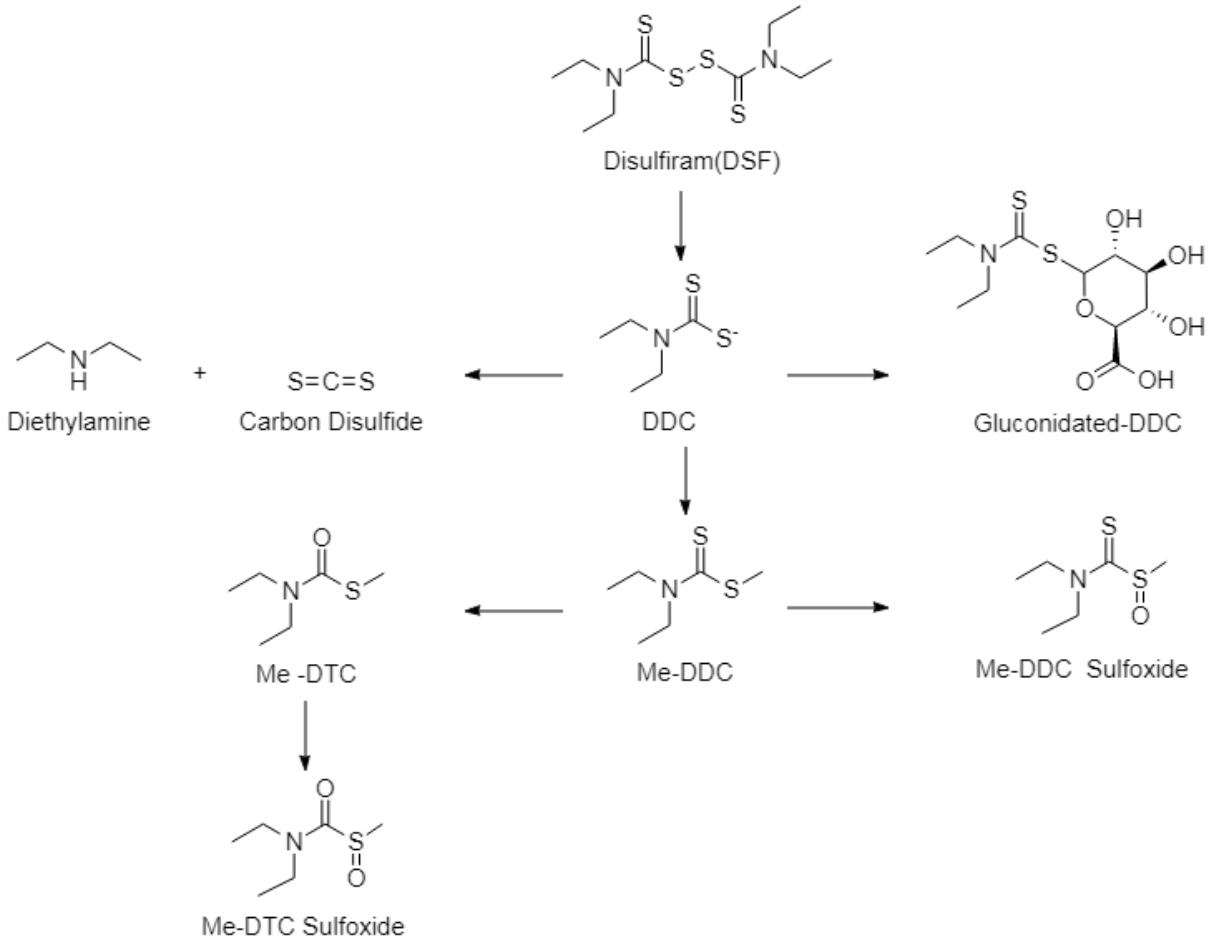

Figure 4. *DSF metabolism [37,44,54,72,73].*

Noteworthy, the anticancer activity of DSF is substantially increased in the presence of copper ions Cu^{+2}(copper-dependent activity) [49]; the concentration of copper ions is higher in cancer cells than in normal ones [40]. DSF can be easily metabolised into DDC which can intracellularly chelate with copper ion as shown in Fig.5 , hence, DSF has approved its selective and specific targeting toward cancer cells [48]. Unless the thiol groups of DDC were methylated or oxidised, blocking the copper chelating activity with it [54].

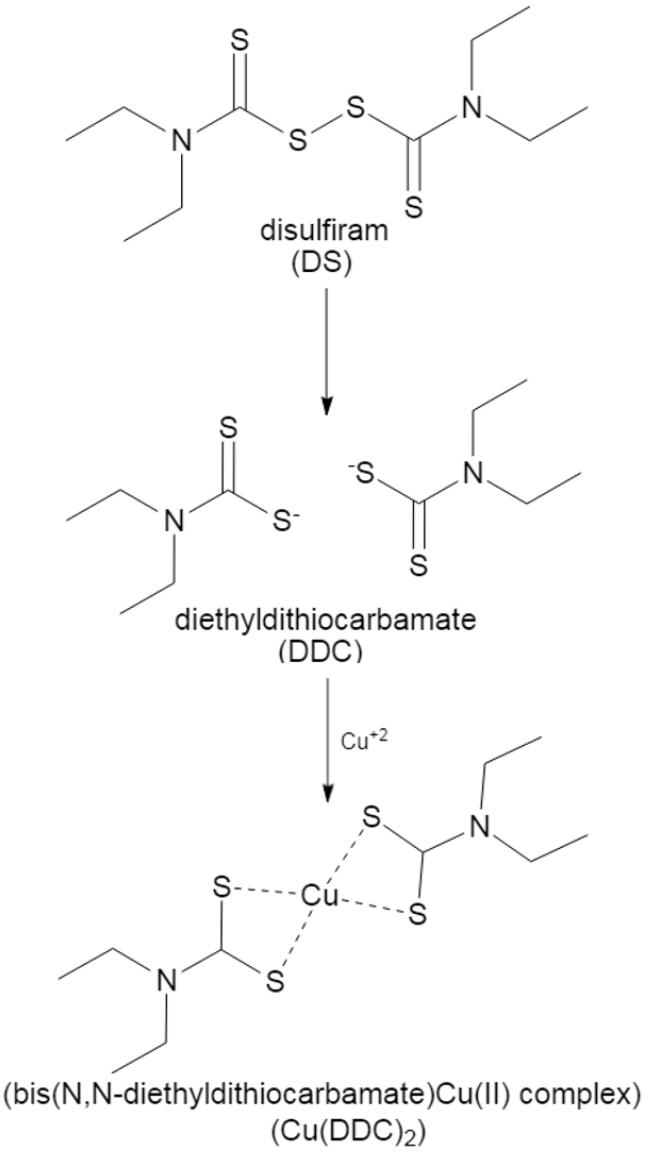

Figure 5. *Chelation of DDC with Cu(II).*

1.6. Chemistry of Copper and Copper Complexes

Copper is an element with atomic number 29, it can be found in different oxidation states and complex structure, among the different ions, two are widely common in biological systems, Cu^{+1} and Cu^{+2} [74,75].

Cu^{+1} is a diamagnetic ions that ends with d^{10} configuration, and can form different complex structure with different coordination number (C.N) [75,76]. Cu^{+2} ions have a d^{9} configuration, and hence it is paramagnetic. Some of Cu^{+1} and Cu^{+2} complex structure are shown in figure 6.

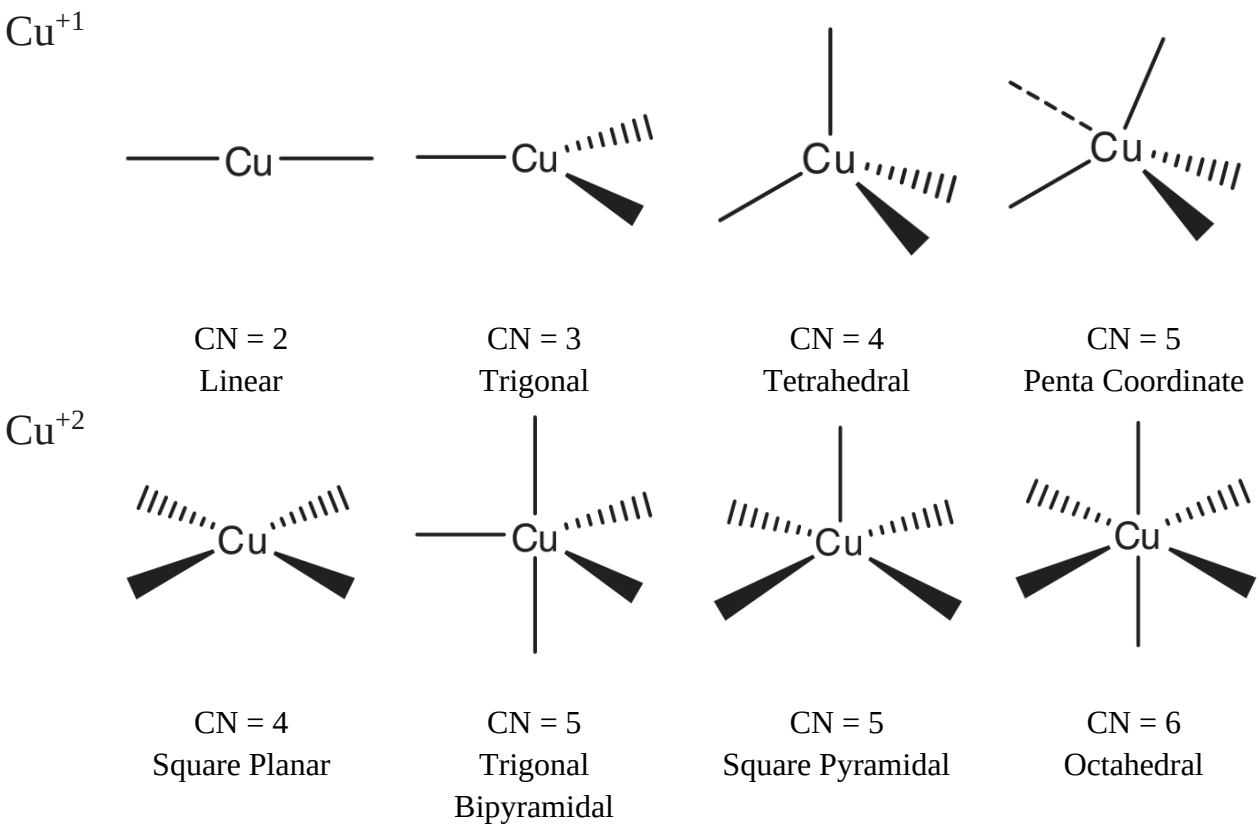

Figure 6. *Copper ion's complex structure base on its coordination number.*

Wide range of different types of ligand (monodentate - hexadentate) can form complexes through nitrogen, oxygen, or sulfur [76], and what characterise these complexes is that they have remarkable stability compared with other metal ion complexes [62].

1.7. Biology of Copper and Copper Complexes

Copper is one of the trace elements essential in many biological activities (mostly related to proteins and enzymes) because of its ability in redox reaction (oxidation-reduction reaction). The main role of copper is promoting the growth and development of connective tissues, energy production, iron metabolism, central nervous system function, immune system, and other functions [78-80].

In the human body, many proteins, enzymes, and transporters are specialised in storing and transporting copper ions in limited quantities to different tissues and cells; thus, preventing accumulation and regulating its homeostasis, as its deficiency or excess causes many diseases. The most known diseases are Menkes and Wilson's diseases. The deficiency of copper causes Menkes disease, where excess and accumulation of copper causes Wilson's disease [81,82]. An example of these regulating proteins is metallothionein protein, which is responsible for storing metal ions like copper and maintaining homeostasis [79,80].

On the other hand, many proteins and enzymes are activated in the presence of copper ions, called copper metalloenzymes. Copper metalloenzymes do crucial biological processes. Some examples include ceruloplasmin (C.P), which is an enzyme and a carrier for about 65%-70% of copper [79], its role is oxidising ferrous(Fe^{+2}) ions to ferric (Fe^{+3}) ions, so the iron can bond with transferrin, and transported through the blood to various tissues in the body [80]. Cytochrome c oxidase (CCO), the enzyme involved in the final step in cellular respiration electron transport

chain in the mitochondria, produces ATP. Its role is to reduce an oxygen molecule with 4e- and 4 protons two water molecules [83]. Cu/Zn superoxide dismutase (SOD1), which catalyses the breakdown of superoxide O_2^- ions to O_2 or H_2O_2, preventing tissue damage [80]. Lysyl oxidase (LOX) is an key enzyme for forming connective tissues by crosslinking collagen and elastin [84,85]. Tyrosinase, an enzyme that catalyses the conversion of tyrosine amino acid to dopaquinone by oxidation, is the first step in melanin production [74]. Dopamine β-monooxygenase(DβM), which catalyses the formation of norepinephrine, is an organic compound that resembles adrenaline in its function [74]. Copper containing amine oxidase (CuAO), a family of amine oxidase catalyses the oxidation of amines to aldehyde, hydrogen peroxide, and ammonia [86], is an example of diamine oxidase (DAO), that catalyse the diamine oxidase of histamine and putrescine [74,87]. Angiogenin (ANG), a protein able to stimulate the development of new blood vessels, is interestingly related to copper ions bioavailability, where the presence of copper ions enhances its activity [88,89]. Moreover, more enzymes and proteins, copper homeostasis affect their activity.

Copper ions have approved its relation with the cancer cells. Several studies reported elevated concentration of copper in various cancer cells comparing with normal cells [90-95]. Also, many studies related the ability of angiogenesis processes in tumour cells with a specific amount of copper as an essential cofactor [96-98]. Therefore, one of the strategies used in various studies for treating cancer, was using anti-copper drug used to treat copper-related diseases like Wilson's disease, preventing angiogenesis [99-101].On the other hand, the antiangiogenic activity of proteasome inhibitor has been approved [102,103], which selectively induces the apoptosis of tumour cells [104-107], and the effectiveness of some organic copper complex in inhibition of

proteasomal chymotrypsin-like activity inducing apoptosis, and its selectivity toward tumour cells have been reported [91].

1.8. Stability of Disulfiram and Cu $(DDC)_2$ Formulations

Bis (N, N-diethyldithiocarbamate) Cu (II) complex (Cu $(DDC)_2$) is a complex combined by disulfiram metabolite diethyldithiocarbamate (DDC) as a bidentate ligand with copper Cu^{+2} ions. A very stable complex gained its stability from its resonance structures between the two sulfur atoms, and due to the presence of the nitrogen atom with its lone pair, the resonance stability is further increased [44,108].

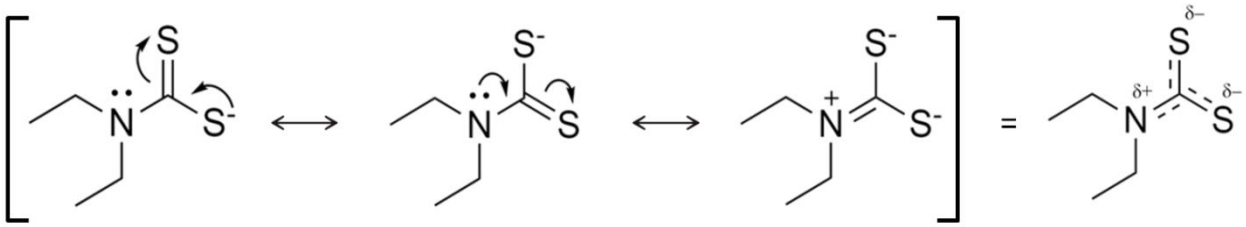

Figure 7. *Resonance structure of DDC. In the first structure, the negative charge of the sulfur atom is delocalised over both the sulfur atom and the carbon atom, resulting in the transition of the negative charge to the other sulfur atom. In the second structure, the nitrogen atom lone pair is delocalised over both the nitrogen atom and the carbon atom, resulting in the third structure where the nitrogen atom is positively charged, and both sulfur atom is negatively charged. The last structure is the combined representation the of three-resonance structure (resonance-stabilised molecule), where the charge is delocalised over the three atoms.*

$Cu(DDC)_2$, like DSF, rabidly degrades in the bloodstream despite its high acid stability [37], as it is a highly hydrophobic complex. The reason why $Cu(DDC)_2$ and other similar complexes become highly hydrophobic after complexation is due to the loss of hydrogen bonding [109], where the chelation of Cu^{+2} with DDC leads to the elimination of hydrogen atom bonded with sulfur, losing the ability to form a hydrogen bond, increasing hydrophobicity [110], and decreasing aqueous solubility [111].

Many studies have proved that the effectiveness of DSF in cancer treatment depends on its copper chelation complex $Cu(DDC)_2$. $Cu(DDC)_2$ is the main drive for the activity of DSF in ROS generation [54,112], UPS inhibition [111], angiogenesis inhibition [67], JNK and P38 activation, NF-kB inhibition [113], and finally act as chemo and radio-sensitizer [69,114]. However, the activity of DSF in ALDH inhibition is controversial; it is suggested that ALDH inhibition is $Cu(DDC)_2$ dependent [115], while others proved that the methylated metabolite plays a crucial role [72].

Chapter Two:

Literature Review

2.1. Literature Review

Due to the high rate of metabolism of DSF and $Cu(DDC)_2$ in blood circulation, their anticancer activity is compromised and needs special consideration in delivery to prolong bioavailability; hence, enhancing their anticancer activity. Nanoencapsulation is an efficient strategy for delivery to maintain their stability in vivo, improve their therapeutic efficiency, and efficiently target cancer cells [26,116,117].

Among nanotechnology techniques that have been used to increase the efficacy of DSF for treating cancer are nanocrystals, polymer-based, lipid-based, and non-polymeric (inorganic) nanoparticles [118,121]. Polymer-based approaches are the most common technique investigated for delivering DSF, including the development of polymer nanoparticles, micelles, and nanogel. Lipid-based nanoparticles include the formation of liposomes in different techniques. Among the non-polymeric or inorganic technique that have been used is silica-based nanoparticles and hollow mesoporous Prussian blue (HMPB)-based Nanoparticle [122,123]. Table 1 summarises some of the studies that have used nanoscience to deliver Disulfiram.

One of the most used techniques for drug targeting delivery is polymer-based nanoparticles, specifically biodegradable polymers. All the desired properties in a polymeric nanoparticle drug delivery system, starting from the particle size, biocompatibility, biodegradability, drug loading and encapsulation, good pharmacokinetic property, to controlled drug release, can be achieved by a variety of modifications including copolymerisation or block copolymerisation for enhanced therapeutic efficiency [124]. For example, utilisation block copolymerisation to produce polymeric micelles, containing both hydrophobic and hydrophilic parts, with the unlimited modification that can be applied have a remarkable ability for poorly soluble or toxic

drugs to be encapsulated and delivered [6,125]. Cationic polymers with amine functional group, anionic polymers with hydroxyl or/and carboxylic acid groups, and finally natural polymers that can be modified to possess either positive or negative charge offer great potential encapsulate the aimed drug [124]. Polymeric nanoparticles also can specifically target specific types of tissues, cells, or even organelles, after modification with different ligands, reducing the side effects of chemotherapy to normal cells and tissues, and minimising the dosage for patients[124]. Furthermore, some of these modified polymeric nanoparticles have a pH, reduction, thermo, and light drug release response [126,127].

Another drug delivery system has been studied and developed since the 90s, which is the green synthesised biodegradable solid lipid nanoparticles (SLNs) [128,129]. it is the most nanomedicine class approved by FDA; due to its biocompatibility and high bioavailability [15], it is also nontoxic, with easy formulation production [128]. The stability of the lipid N.P.s system is altered by its size and surface charge [130]. Some SLNs colloidal structures are micelles and liposomes [131,132]. Liposome nanoparticle, an exceptional harmless drug carrier system for the transfer of both hydrophobic and hydrophilic drugs with a high loading efficiency [18]. These liposomes can also be hybridised with other nanoparticles to enhance the different therapeutical activities like enhancing its circulation in the blood [133]. Many developed liposome systems have proved their efficiency in different therapeutic fields; examples are magnetic liposomes [134], liposomes in photodynamic therapy [135,136], liposomes modified with cell-penetrating peptides [137], and cytoskeleton-specific immunoliposomes [138]. Another characteristic feature of these nanoparticles is their available site for binding, where the drug and nanoparticles can be encapsulated inside the liquid core, embedded between the two lipid bilayers, or adsorbed on the outer surface of the liposomes [18]. This allows for a wide

variety of drug types and nanoparticles to be efficiently delivered. Inorganic N.P.s have numerous N.P.s types with various synthesis methods [139]. Inorganic N.P.s include carbon nanotubes, noble metal, silver-based, gold-based, magnetic ZnO, copper oxide, and fluorescent N.P.s [140,141]. These nanoparticles can provide several applications in oncology, including imaging, drug delivery, and enhancement of radiotherapy [141,142]. What distinguishes inorganic N.P.s is their biocompatibility, high stability, hydrophilicity, and non-toxicity compared with other N.P.s [143]. One of these inorganic N.P.s that have been used in DSF delivery is mesoporous silica. Lots of properties that distinguish mesoporous silica nanoparticles have attracted researchers' attention, as its simple fabrication gives a highly stable, bifunctional surface with the ability to specifically functionalised the inner or outer surface for different drugs, and the high surface area leading to a high drug loading efficiency, and most importantly, the ease to get a uniform pore size with an adjustable pore size as needed [144-146].

W. Chen has reduced the drug-resistant prostate cancer and other cancer types by its $Cu(DDC)_2$ micelle N.P., with a drug-loading efficiency close to 100% [147]. While P. Banerjee has successfully delivered DSF to breast cancer cells with a 48.24% tumour growth inhibition rate and increase circulation time in the blood by the synthesis of increased circulation time in the blood by synthesising and increasing circulation of increased circulation time in the blood time in the blood by synthesising TPGS-DSF-NLC [148]. Encapsulation efficiency of DSF up to 96.6 ± 0.24% with a drug-loading capacity of 36.23 ± 0.9% was achieved through paclitaxel-disulfiram nanocrystals (PTX-DSF Ns) synthesised by I. Mohammad. This nanocrystal drug has approved its efficiency to improve the apoptosis of lung cancer cells [149]. H. Fasehee has successfully inhibited and reduced the cancer cells growth of breast cancer using folate-receptor-targeted PLGA-PEG NPs (DS-PPF-NPs). DS-PPF-NPs effect was studied by performing on

five-week-old female BALB/c mice [108]. More research and nanoparticles types used to deliver DSF are summarised in Table 1.

The utilisation of nanoparticles for targeted drug delivery has achieved several advantages and improved drug efficacy [150]. Nanoparticles which are characterised by their high surface area; and high drug loading efficiency can also control drug release [151].Toxic/nontoxic drugs, whether they were hydrophobic or hydrophilic, can also be delivered to the target site [118]. Furthermore, nano-drug has approved its efficiency in overcoming drug resistance [152]. Choosing the exemplary nanoparticles with the best formulation is a challenging issue. A set of essential attributes can be a suitable size and shape [15], prolonged blood circulation time, biocompatibility, biodegradability, cell penetration efficiency [153], and low toxicity. Size around 100 nm is the best, as it can achieve EPR (Enhanced Permeability and Retention) effect[154,155]. Nanoparticle with greater size has short circulation time, while 10 nm or less can damage normal cells [152,156].

Lipid nanoparticles, including liposomes, micelles, and nanoemulsion, mimic the cell biological membrane; thus, it has special biocompatibility and biodegradability [129,131]. Also, some polymers that are biodegradable are gaining a lot of attention, especially PLGA (Poly (lactic-co-glycolic acid)). FDA approves PLGA, and it has low toxicity as it degrades to nontoxic materials [157,158].

Table 1. *DSF nanotechnology-based delivery.*

Nanoparticle Type	Component	Particle Size(nm)	Encapsulation Efficiency (%)	Drug Loading (%)	Target	Ref
Polymeric Nanospheres and Nanocapsules	DSF/PLGA /PEG-NH_2-Folate	204	59.62±0.66	5.42±0.06	Breast Cancer	[108]
	DSF/PLGA	136.2±62	78.92±2.16	27.67±3.47	Liver Cancer	[159]
	DSF/PLGA	165	58.85 ± 1.01	5.35 ± 0.03	Breast Cancer	[160]
	DSF/PLGA/PVA	145.2-208.4	69-94	_	Lung Cancer	[28]
	DSF/PLGA/PEG/PVA/Folate	204	_	_	Breast Cancer	[161]
	DSF/PLGA/Polysorbate 80	120	_	24	Liver Cancer	[162]
	DSF/PDA-PEG/LBA	30.05 ± 0.42	_	_	Tumour	[163]
	DSF/mPEG-PCL/PCL or mPEG-PLA/PLC	100.5 ± 10.8	_	5.21	Liver Cancer	[164]
	DSF/mPEG-PLGA/PCL	79.0 ± 9.3	51	5.1	Breast Cancer	[165]
	DSF/PCL/mPEG/BLG/DOX	121.4 ± 0.7	DOX: 95.6 Cu $(DDC)_2$:98	DOX: 4.78 Cu $(DDC)_2$:4.9	Breast Cancer	[166]

Nanoparticle Type	Component	Particle Size(nm)	Encapsulation Efficiency (%)	Drug Loading (%)	Target	Ref
	DSF/PGA/PEG/CisPt	31.4 ± 2.6	_	19.5	Lung Cancer	[167]
	DSF/mPEG-PLGA	81.74 ± 3.3	92.1	18.47	Brain Cancer	[168]
Nanogel	Cu+2/OPDMA	160	_	_	_	[169]
Micelles Nanoparticle	DSF/PEG-b-PLL/PTX/DMA	138 ± 8.5	85.7 ± 2	1.97 ± 0.8	Breast Cancer	[170]
	DSF/DOX/SMA/ADH	88.58 ± 4.12		5	Breast Cancer	[171]
	DSF/PEC	200	DDC: 17.3 Cu^{+2}: 30.7	10	Lung Cancer	[172]
	DSF/Cu^{+2}/PEG	70-60		~100	Prostate Cancer	[147]
	DSF/SMA	160	75.4	7.5	Lung Cancer	[173]
Lipid Nanoparticle	DSF/ lipoid/Kolliphor HS-15/TATp/PGA-g-PEG	93.7	_	3.59 ± 0.36	Tumour	[174]
	DSF/TPGS/tween 80/Precirol ATO5/Labrafac Lipophile WL1349/ lecithin	188.6 ± 1.5	80.7	_	Breast Cancer	[148]

Nanoparticle Type	Component	Particle Size(nm)	Encapsulation Efficiency(%)	Drug Loading (%)	Target	Ref
Liposome	DSF/Cu^{+2}/DSPC-Chol(55:45)	_	_	28.5	Brain Cancer	[175]
	DSF/Cu^{+2}/PEG/Oleate	109.6	_	4	Tumour	[176]
	HSPC/DDPC/DSPE-PEG200 / DSF/Cu^{+2}	80-100	80%	60%–68%	Colorectal Cancer	[177]
Nanoemulsion	DSF/ethyl oleate/Tween 80/Transcutol HP/DSPE-PEG 2000/	63.4 ± 1.1	_	_	Glioblastoma	[178]
Nanocrystal	DSF/Cu^{+2}/PEG/H_3PTC	207.3	_	2.41	Tumour	[179]
	DSF/DOX/LDH/PEG-PLG/HA	213.2±0.95	DOX: 68.6 $Cu(DDC)_2$:98	DOX:4.52 $Cu(DDC)_2$:10.51	Liver Cancer	[180]
	DSF/PTX/β-LG	162	96.6 ± 0.24	36.23 ± 0.9	Lung Cancer	[149] [181]
Silica Based Nanoparticle	DSF/Cu+2/PEG/Mesoporous Silica Nanoparticles	172.5	_	18.8	Breast Cancer	[182]
Hollow mesoporous Prussian blue (HMPB)-based Nanoparticle	DSF/Cu^{+2}/PVP/HMPB	144.5	_	_	Breast Cancer	[183]

2.2. Aim and Objectives

This project aims at:

- Repurposing of DSF as anti-cancer drug.
- Synthesis and characterization of $Cu(DDC)_2$ by FT-IR, Uv-vis, and zeta potential.
- Delivering poorly soluble $Cu(DDC)_2$ to the cancer cells; via encapsulation by o/w emulsion, to enhance drug blood circulation, drug release, and selective cytotoxicity.

Chapter Three:

Materials and Methods

3.1. Chemicals

Sodium diethyldithiocarbamate trihydrate, copper sulfate pentahydrate, dichloromethane (≥99.8%), Polyethylene glycol 8000 (PEG), Polycaprolactone 80,000 (PCL), castor oil, Tween® 80, Fatal Bovine Serum (FBS), and Trypsin were purchased from Sigma Aldrich. Soybean lecithin was a gift from commercial company. A549 cells was purchased from ATCC.

3.2. Instruments

Cu $(DDC)_2$ was characterised by Perkin-Elmer, Spectrum Two, FT-IR spectrometer that has a range of (4000–400 cm^{-1}). Cu $(DDC)_2$ concentrations were measured by an Aqualab Company UV-Visible line 9100 spectrophotometer that has a photometric range of 300 – 1100 nm. Nanocapsules (NC) have been produced using Ultrasonic processors Sonics, Materials VC-750-220, Fisher Scientific. Other instruments are Elmasonic S 30 (H) water bath sonicator, Medifuge™ Small Benchtop Centrifuge, disposable PD 10 desalting columns GE17-0851-01, and shaking incubator (LSI-3016A).

3.3. Methods

3.3.1. Preparation of Copper Diethyldithiocarbamate (Cu $(DDC)_2$)

Cu $(DDC)_2$ was prepared by directly pouring 100 ml of 0.055 molar copper sulfate pentahydrate solution (blue colour) into 100 ml of 0.055 molar disulfiram solution (colourless), forming a dark brown precipitation. The formed precipitate was filled into 13 ml falcon tubes, washed by distilled water and centrifuged three times, then dried at 40º C. and collected as shown in Fig.8. Weight of the collected $Cu(DDC)_2$ was 1.875 g.

Figure 8. *$Cu(DDC)_2$ powder.*

3.3.2. Preparation of Polymeric Nanocapsules

Dichloromethane was used as an organic solvent, whereas deionized water as an aqueous solvent. Lecithin as a lipophiic emulsifier with HLB equals 7-10 [184]. Tween 80 as a hydrophilic emulsifier with HLB equals 15 [185]. The total HLB was 11.09 where this value favours o/w emulsion.

The prepared Cu $(DDC)_2$ was dissolved in castor oil (50 mg $Cu(DDC)_2$/4 g castor oil). For oil-in-water (o/w) emulsion preparation, the organic phase was prepared by three steps. Firstly, 25-30 gm of lecithin was added to 3 ml of dichloromethane and mixed in a bath sonicator producing a pale-yellow colour solution. In the second step, PEG and PCL were dry blended in three different ratios, 25:75, 50:50, and 75:25, to form a total of 20 mg polymer and added to the previous solution and bath sonicated until the polymers were dissolved. Afterwards, 100 mg of Cu $(DDC)_2$/castor oil (1.25mg drug) was added to the previous solution and covered; then bath sonicated till the drug was fully dissolved.

For the aqueous phase preparation, about 20 mg tween 80 was added to distilled water for the aqueous phase then shaken till a soupy solution formed. Finally, o/w emulsion was prepared by the addition of the organic phase to the aqueous phase and probe sonicated for 180 sec at 20%

amplitude forming a creamy colour emulsion. The sonicated solution was then stirred by a magnetic stirrer for 2 h to evaporate dichloromethane. The prepared o/w emulsion was stored at 4º C.

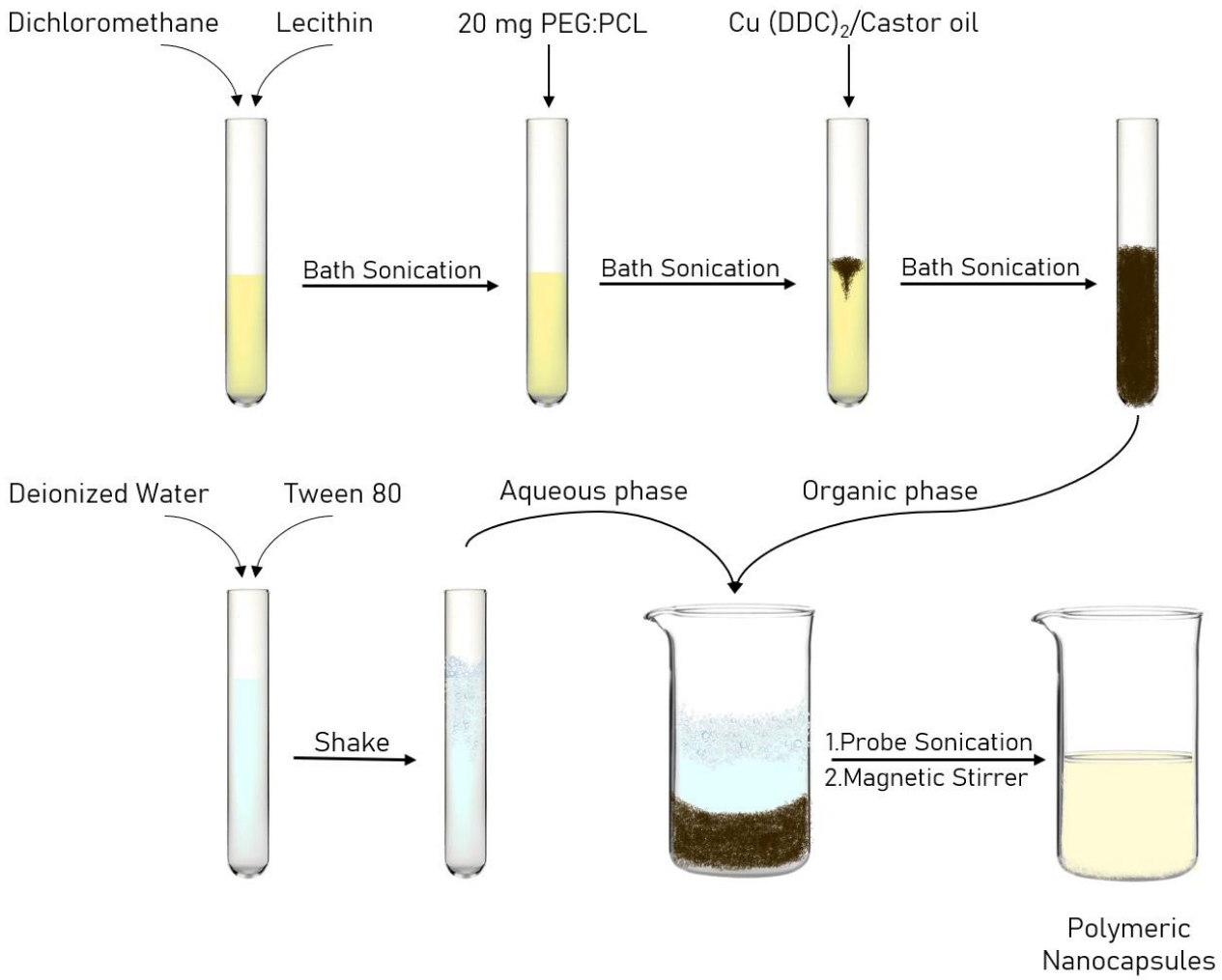

Figure 9. *Polymeric nanocapsules preparation three stages. Firstly, organic phase preparation by mixing dichloromethane, lecithin, PEG, PCL, and Cu(DDC)$_2$/castor oil. Aqueous phase preparation by mixing deionized water and tween 80. Finally, preparation of nanocapsules by mixing the organic phase and aqueous phase using probe sonicator.*

3.3.3. Encapsulation Efficiency

The Polymeric nanocapsules suspension was characterised and investigated for its physicochemical characteristics; namely the encapsulation efficiency.

The percentage of encapsulation efficiency (EE) was measured by applying a previously developed method with adapting some amendments to suit the highly hydrophobic drug. Briefly, the nanocapsule suspensions were purified by a PD-10 desalting column, size exclusion chromatography (GE17-0851-01) and eluted in water to remove any un-encapsulated drug. The samples were centrifuged twice at 10K RPM for 30 minutes, and pellets were collected and incubated in 5 ml dichloromethane for 1 hour at 37 °C, vortexed, and sonicated in a water bath for half an hour to break the polymeric shell. Afterwards, the suspensions were dried under a fume cupboard until all dichloromethane was evaporated and the samples were solidified. The nanocapsule systems were resuspended in 10 ml water and vortexed to dissolve PEG and other hydrophilic components, and centrifuged twice at 10K RPM for 30 minutes. The resultant pellets were collected and suspended in 5 ml dimethyl sulfoxide (DMSO), vortexed and sonicated to dissolve the drug, and centrifuged to remove the undissolved polycaprolactone. The supernatant was collected and read at λ_{271} nm, and the concentration was collected by utilising the calibration curve equation.

The percentages Encapsulation Efficiency (%EE) and Percentage Protein Loading (%LE) of the drug were calculated using the following equation:

$$\%EE = \frac{weight\ of\ Cu(DDC)_2\ encapsulated}{weight\ of\ initially\ added\ drug}\ x\ 100\%$$

$$\%LE = \frac{weight\ of\ Cu(DDC)_2\ encapsulated}{weight\ of\ polymer}\ x\ 100\%$$

Standard curves used for $Cu(DDC)_2$ quantification are presented in Figure 12.

3.3.4. Particle Size Analysis and Zeta Potential

Hydrodynamic size (Z-Average diameter), polydispersity index (PDI) and zeta potential of $Cu(DDC)_2$-containing polymeric nanocapsules were measured using the Zetasizer instrument (NanoZS®, Malvern Instruments Ltd., Malvern, UK). The measurement was performed at 25°C using disposable square polystyrene cuvettes and disposable capillary cells (Malvern Instrument, UK) for (size and PDI) and zeta potential, respectively. The samples were prepared by diluting the suspension by 100 times and vortexing it to obtain homogeneous system in water or 0.09% NaCl for the size and the zeta potential, respectively. Z-Average diameter and PDI were measured with 15 runs within each measurement, while the zeta potential measurement had taken place with 20–25 runs within each measurement. All parameters were measured for freshly prepared samples and 14 days after storage in refrigerator at (4-7 °C). All measurements were carried out in triplicate, and means, and standard deviation (SD) readings of size and zeta potential were calculated for each sample.

3.3.5. Drug Release

After the evaluation of the physicochemical properties of $Cu(DDC)_2$-containing polymeric nanocapsules at different ratio, 25:75 PEG:PCL nanocapsules formulation was chosen to be further studied for release kinetics and other in vitro investigation. $Cu(DDC)_2$ release from the nanocapsules was determined in phosphate buffer saline (PBS), that was prepared according to British Pharmacopea 2014 [186]. 5 batches (6.5 mg drug) of the prepared NC suspensions were

centrifuged and pellets were collected and suspended in 20 ml of PBS vessels and incubated in a water bath shaker LSI-3016A.

5 ml of the prepared NC suspension was centrifuged, and pellets were collected, dried and divided into three parts and added to 1 ml PBS Eppendorf tube and incubated in a water bath shaker (shaking incubator (LSI-3016A)). Ten Eppendorf tubes were incubated to assess the dissolution at 10 different time points: 0.5 hour, 1 hour, 2 hours, 4 hours, 12 hours, 24 hours, 2 days, 7 days, 14 days, and 24 days. At each time point, each tube was taken and centrifuged, and three layers were obtained; oil droplets on the top, supernatant, and pellets. Oil droplets were collected reconstituted in 0.5 ml DMSO, vortexed and measured by UV at λ_{271}. For the first 4 samples the concentration was very low and below the lower limit of detection; thus, pellets were collected, reconstituted in 1 ml DMSO, vortexed for 1 min, and centrifuged. Afterwards, supernatants were collected and 10-fold or 100 ml diluted, depending on the concentration, and measured by UV at λ_{271}.

3.3.6. Serum Stability of Encapsulated $Cu(DDC)_2$ in FBS

The stability of free and encapsulated $Cu(DDC)_2$ was studied in Fetal Bovine Serum (FBS) to investigate how efficient the encapsulation process in protecting $Cu(DDC)_2$ after IV injection. Half ml of the polymeric nanocapsules suspension was added to 2 ml FBS after heating both of them at 37 °C an incubated in a shaking water bath at 37 °C and 100 rpm. A mixture of , 50 µL of 2mg/mL $Cu(DDC)_2$ in DMSO, 450 µL of deionised water, and 2 mL of FBS was prepared and heated at 37 °C to investigate the stability of free $Cu(DDC)_2$ in FBS. The study was conducted for a total of 4 hours and samples aliquots were collected at 0, 0.25, 0.5, 1, 2, 4 hours time points. At each time point, 200 µL of each mixture (free drug and nanocapsules mixture) was added to 700 µL of methanol and vortexed for 1 min. Each mixture solution was centrifuged

at 10,000 rpm for 10 min. Afterwards, solution was set to dry for 2 hours under fume cupboard to evaporate methanol, and 0.5 ml DMSO was added, vortexed and centrifuged to dissolve the drug and get rid of all non-soluble parts. Finally, λ_{271} of the solutions was read by UV-vis spectrophotometer. The same steps were followed; however, water was used instead FBS as a positive control. The positive control was used a 100% for the stability calculations.

3.3.7. Cytotoxicity Study

A549 human lung carcinoma cells (A549, ATCC®, CCL-185™) were cultured in Advanced RPMI 1640 medium supplemented with, 1% penicillin-streptomycin 10% fetal bovine serum (FBS) and 1% L-glutamine, in 5% CO2 and 95% air, at 37 °C. Cell confluents were split at 1:4 twice a week.

The A549 cells were seeded in 96-well plates at 5 $\times 10^3$ cells per well overnight. Cells were incubated with $Cu(DDC)_2$, NC-$Cu(DDC)_2$ or equivalent concentrations of blank NC in complete medium for 24 hours, 72 hours. MTT assay was applied to determine the viability of treated cells. At the end of each incubation period, the supernatant of each well was removed and replaced with 120 μL of MTT solution prepared by 1:6 dilution of 5 mg/mL in PBS in complete media. Cells were incubated for 3 hours at 5% CO_2 and 95% air at 37°C. Next, 200 μL of DMSO was added to solubilise the formazan and was incubated for 5 mins at 37°C. The absorbance was read using an FLUO star OPTIMA plate reader (BMG Labtech) at 570 nm. Percentage cell viability was calculated using the equation below and expressed as mean ± standard deviation (SD).

3.3.8. Statistical Analysis

All results are presented as mean ± standard deviation (SD). Paired sample T-tests were performed, and the one-way analysis of variance (ANOVA), as appropriate. The two-tailed significance (p-value) was determined. Statistical significance was considered as p-value$\leq$ 0.05.

Chapter Four:

Result and Discussion

4.1. Preparation and Characterisations of $Cu(DDC)_2$

The obtained brittle powder of $Cu(DDC)_2$, has a dark brown colour and high stability; as it has no reactivity with air or water, it can be saved easily. The FTIR study was done by preparing a semi-transparent, light brown disk of KBr-$Cu(DDC)_2$. As $Cu(DDC)_2$ has low solubility in water, the UV study was done by dissolving the prepared sample in DMSO to several concentrations. The surface of produced N.P.s was modified with two biocompatible nontoxic polymers PEG and PCL, which can degrade in vivo easily [6]. PEG that has the ability to increase the drug delivery system stability, hydrophilicity, and prolong circulation lifetime of N.P.s system; as it cannot be recognized by immune system monocytes and macrophages[187,188].

4.1.1. FT-IR Study

FT-IR spectrum was obtained using Perkin-Elmer, Spectrum Two, FT-IR spectrometer that has a range of (4000–400 cm^{-1}). A small amount of $Cu(DDC)_2$ was mixed with potassium bromide (KBr) and grinded. Then using KBr Quick Press Accessory a small disc was made, and placed in the spectrometer.

The FT-IR spectrum of $Cu(DDC)_2$ is shown in fig.10, it shows a strong absorption band at 1507 cm^{-1} referring to C-N bond [189]. This peak emphasises the resonance stabilisation between carbon and nitrogen atoms; where the C-N single bond absorption is between 1342-1266 cm^{-1}, and C-N double bond absorption is between 1690-1640 cm^{-1}. The weak absorption band at 2981 cm-1 refers to the C-H stretching[190].

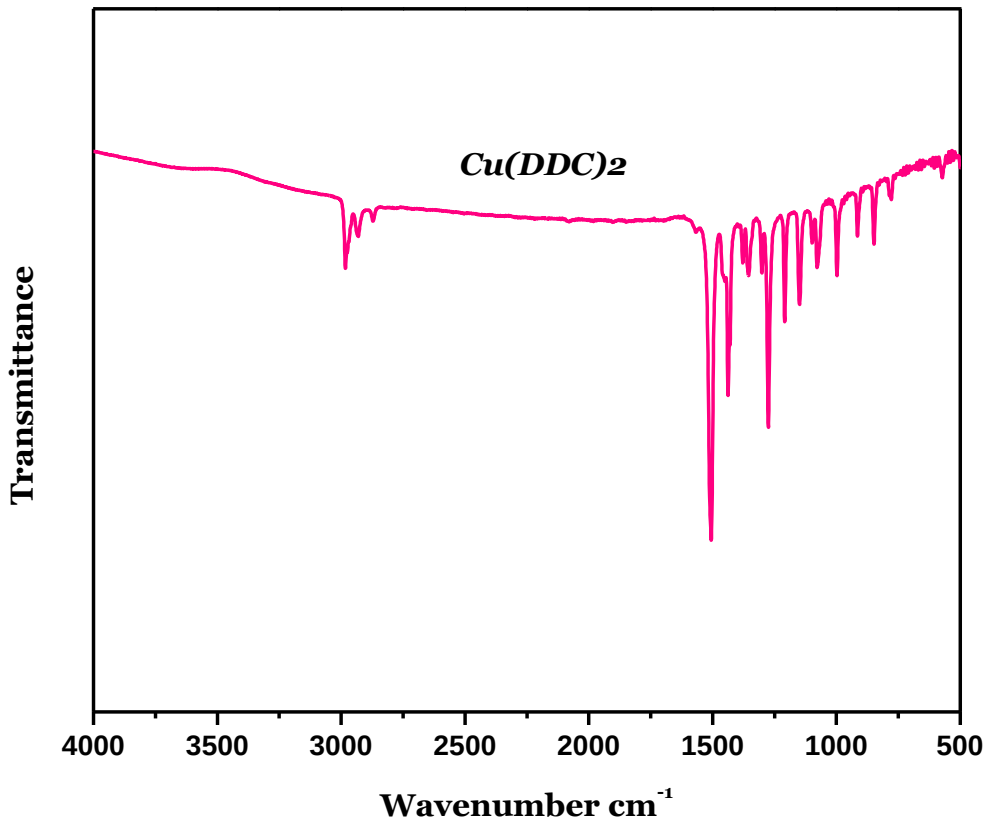

Figure 10. *FT-IR spectrum of Cu(DDC)$_2$.*

4.1.2. UV-Vis Spectrophotometer

Fig. 11 shows the absorption spectrum of Cu(DDC)^2 at different concentrations. As shown in fig. 11, the strong peak appears at 271 nm, and the broad peak around 435 nm which indicate the copper ions in the complex [175,191]. Cu(DDC)$_2$ was dissolved in DMSO to different concentration, ranges from 0.5 to 12 ppm, λ_{max} at 271 nm for these concentration has shown a linear relationship in the calibration curve represented in fig.12, with a regression coefficient (R^2 = 0.9761).

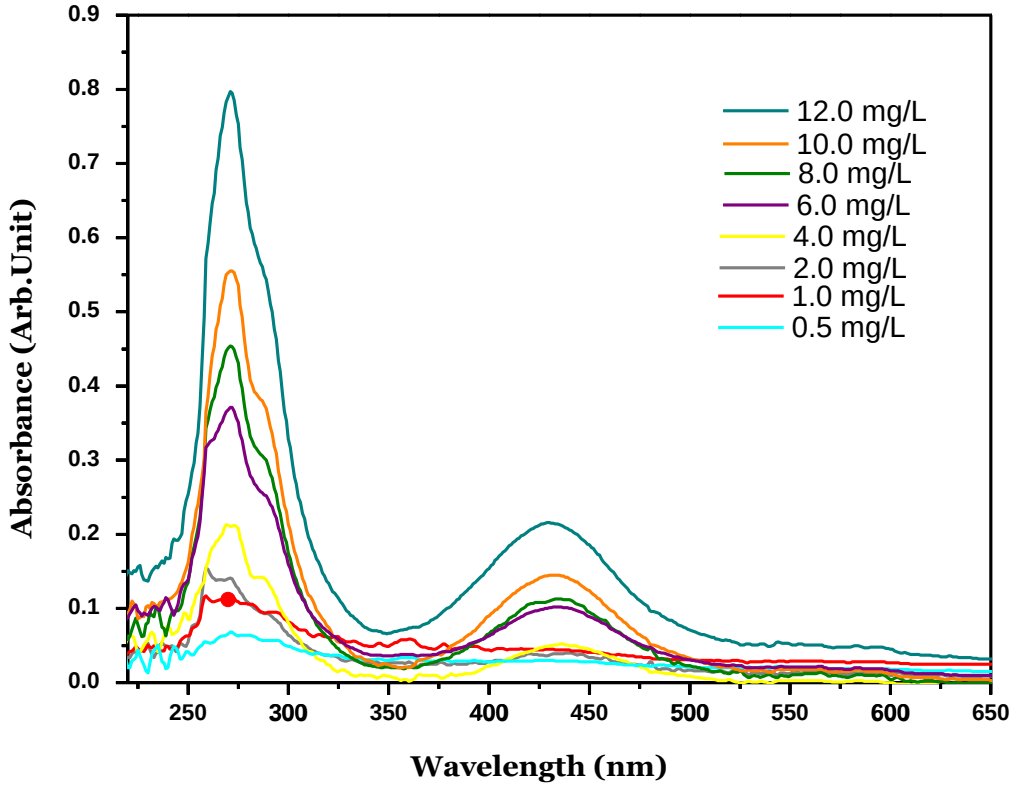

Figure 11. *UV-Vis spectra for $Cu(DDC)_2$ concentration between 0.5 mg/l and 12.0 mg/l.*

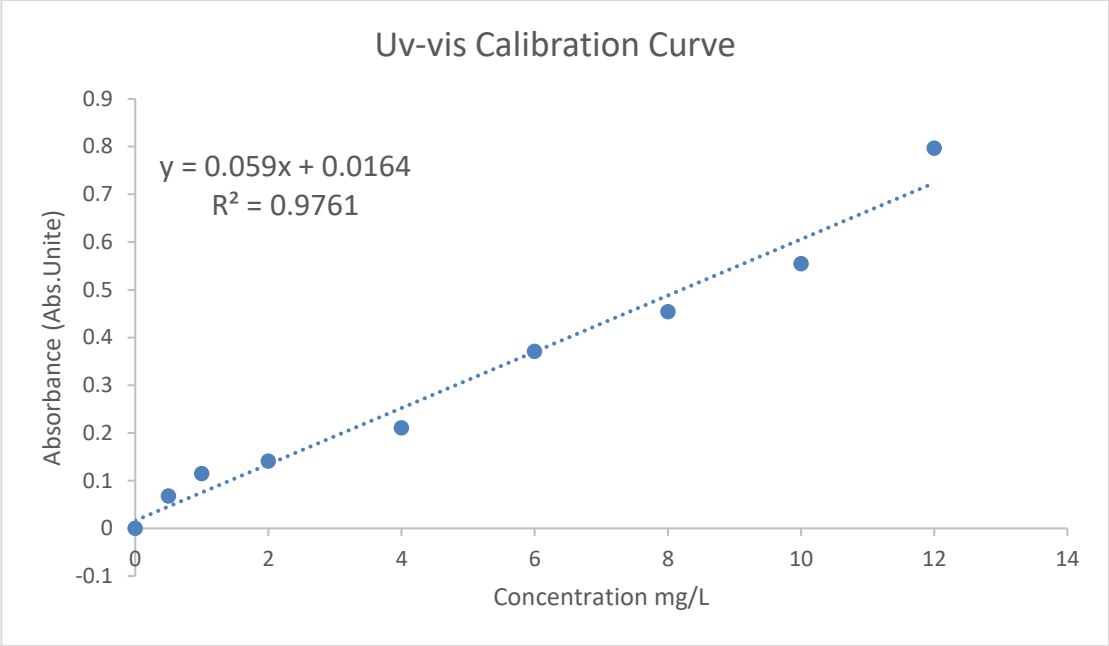

Figure 12. *The calibration curve of* $Cu(DDC)_2$.

4.2. Physicochemical Characterisation

Using zetasizer, thre of the affecting factors that influence the stability of NP are characterized, which are size, PDI, and zeta potential. All the three values for the different PEG:PCL ratios are summarized in Table 2. Among the three ratios of PEG and PCL that were studied, the 25:75 ratio has the most preferable readings, where the particle size ranges around 88.7 nm when freshly characterized, and 92.3 nm after 14 days of storage, with a PDI of 0.11 and zeta potential equal -35.7 mV. The other two ratios have shown a wide range between the size reading of freshly prepared and stored samples; indicating lower stability. 50:50 ratio has a size of 97.8 nm for the freshly prepared sample, and 127.9 nm for the stored one, with a PDI of 0.21 and a zeta potential equal to -36.4 mV. Size of 75:25 ratio for fresh sample equals 128.2 nm, while after storage the size becomes 179.8 nm, with a PDI equals 0.42 and zeta potential equal -37.5 mV.

System F2 and F3 are not desired as the observed particle size measured for F2 and F3 nanoparticle, and their higher PDI values indicate lower stability and dispersed particle size

Table 2. *Average particle size, PDI, and zeta potential for different PEG:PCL ratios of N.P.s.*

PEG:PCL N.P.s	Average particle size (nm)		PDI	Zeta potential
	Fresh	After 14 days		
25:75	88.7	92.3	0.11	-35.7
50:50	97.8	127.9	0.21	-36.4
75:25	128.2	179.8	0.42	-37.5

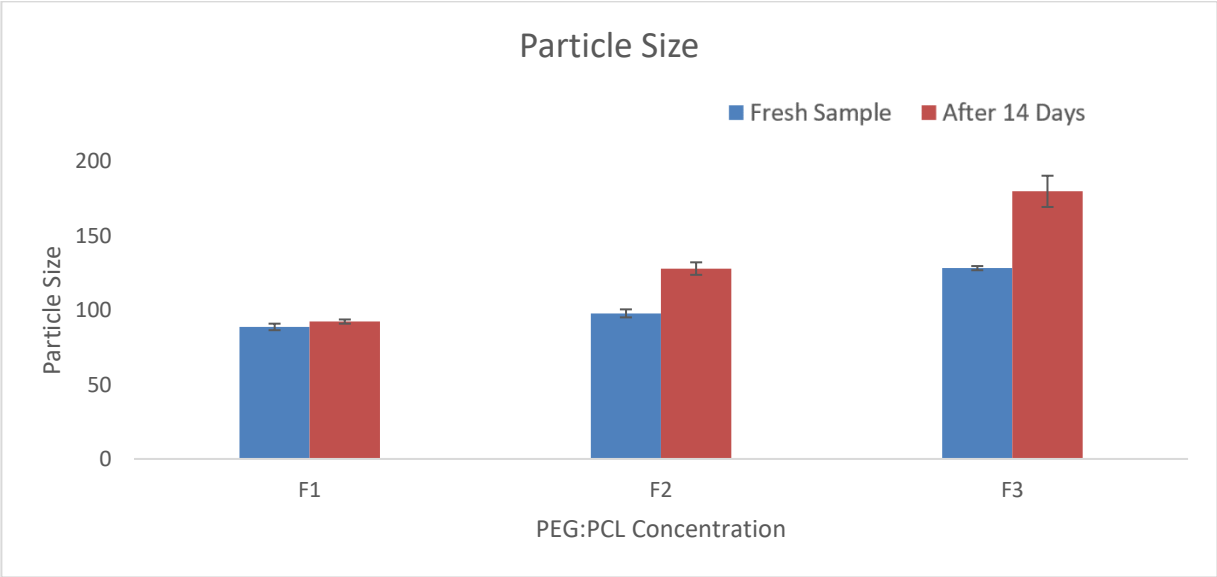

Figure 13. *The particle size of $Cu(DDC)_2$ N.P.s at PEG:PCL different concentration, F_1 (25:75),F_2 (50:50), and F_3 (75:25). The blue column indicates the particle size for the fresh sample, while the red one is for the stored one for 14 days.*

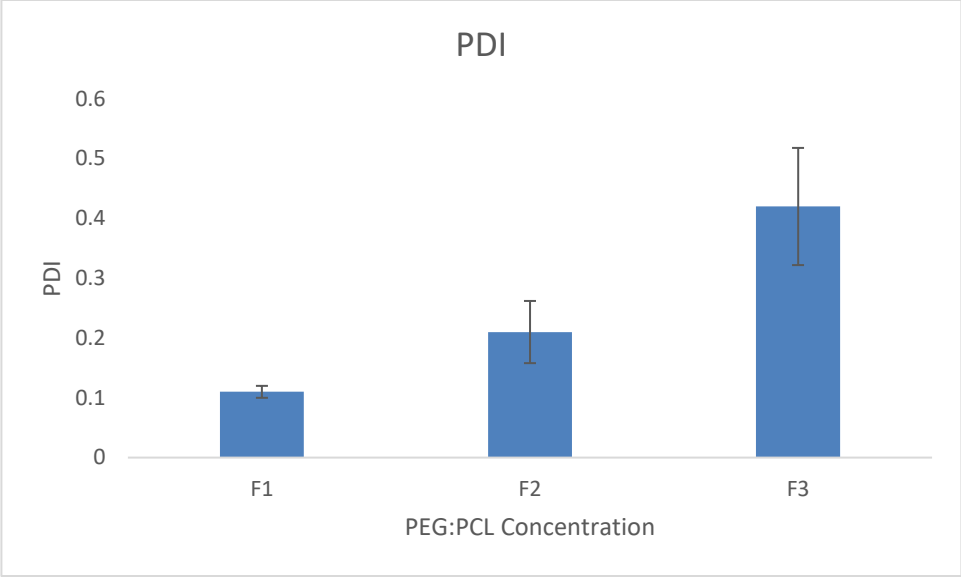

Figure 14. *Polydispersity index of Cu(DDC)$_2$ N.P.s for the three different concentration of PEG:PCL , F$_1$ (25:75),F$_2$ (50:50), and F$_3$ (75:25).*

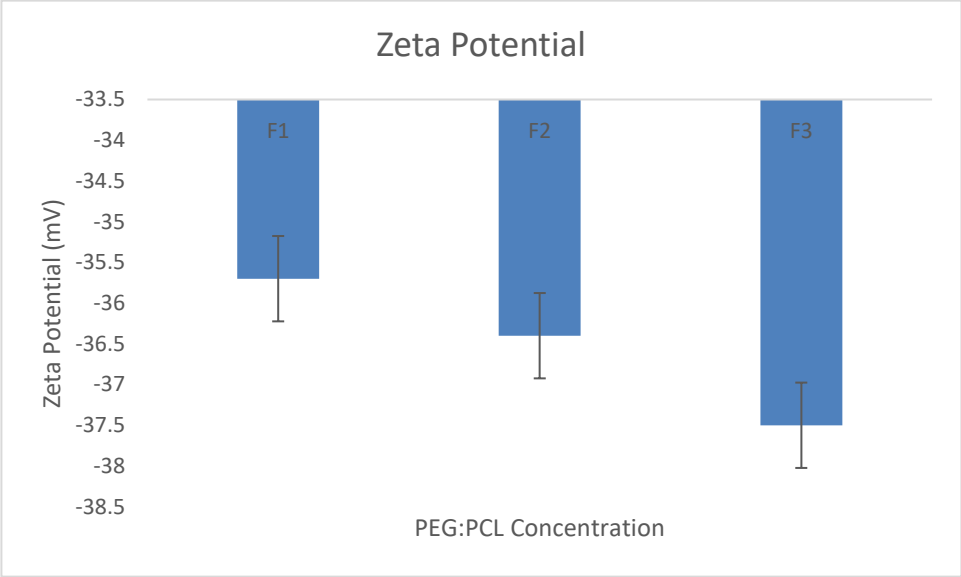

Figure 15. *Zeta potential of Cu(DDC)$_2$ N.P.s for the three different concentration of PEG:PCL , F$_1$ (25:75),F$_2$ (50:50), and F$_3$ (75:25).*

4.3. Serum Stability

A graph and a table showing the stability of each form, encapsulated $Cu(DDC)_2$ (NC), and free drug (FD) in FBS at the various time points is in fig.16 and table 3 below, according to it, the big difference between serum stability in FBS can be observed. Where after 4 hours (240 min) the remaining ratio of FD is 14%, while NC is 65%, relating to the higher stability and solubility of NC; according to the encapsulation and conjugation of the drug with polymers.

Table 3. *The remaining % of free $Cu(DDC)_2$ (FD) and encapsulated $Cu(DDC)_2$ (NC) N.P.s in FBS at various time.*

Time	0 min	15 min	30 min	60 min	120 min	240 min
FD Remaining %	100%	74%	61%	42%	28%	14%
NC Remaining %	100%	94%	92%	88%	75%	65%

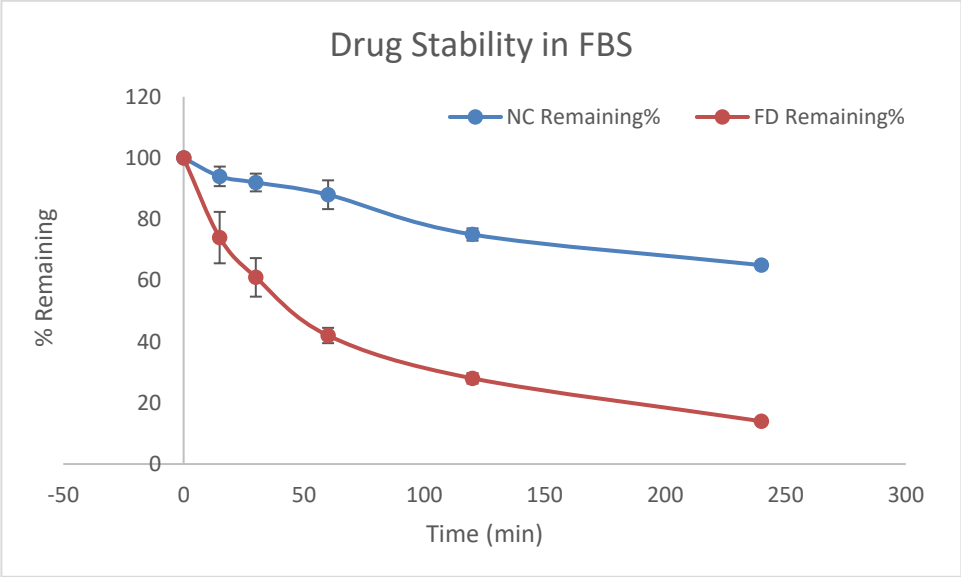

Figure 16. *The stability of free $Cu(DDC)_2$ (FD) and encapsulated $Cu(DDC)_2$ (NC) N.P.s in FBS. The measurement was taken at 0 min, 15 min, 30 min, 60 min, 120 min, and 240 min.*

4.4. Drug Release Studies

Drug release study (fig.17) shows a burst release phase till 24 hours, where 48.63% of the drug is released. A constant slow release is observed for two weeks, where after one week, the percentage release reaches 65.3%, while after two weeks the released drug goes up to 97.6%. Thereafter, extremely slow and negligible drug release is obtained. The drug release study is summarized in Table 4.

Table 4. *Drug release percentage of 25:75 PEG:PCL nanocapsules at time.*

Time	Release%
0 hour	0%
0.5 hour	0%
1 hour	1.12%
2 hour	2.1%
4 hour	18.6%
12 hour	24.6%
24 hour	48.63%
48 hour	54.12%
168 hour	65.3%
336 hour	97.6%
672 hour	98.3%

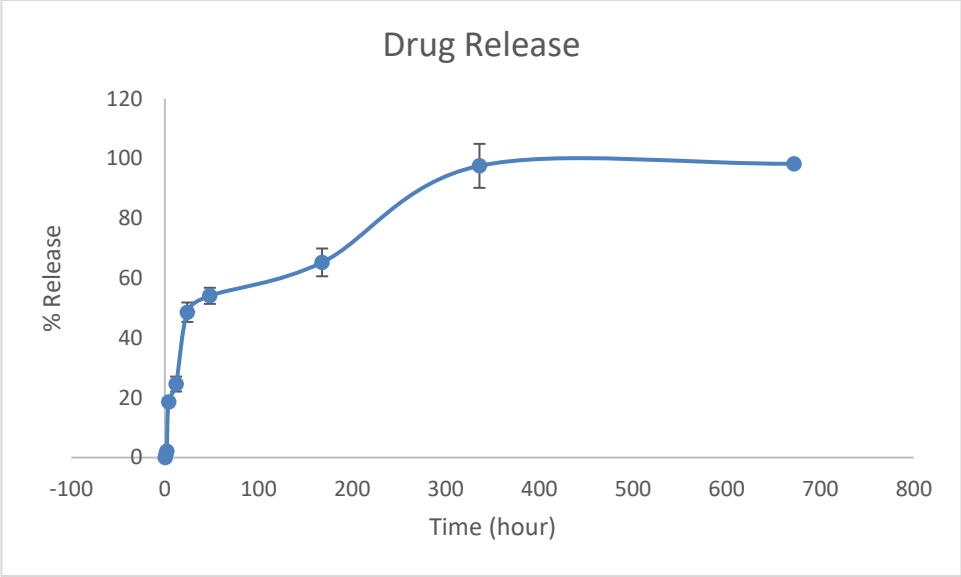

Figure 17. *Drug release of 25:75 PEG:PCL nanocapsules at 10 different time points: 0.5 hour, 1 hour, 2 hours, 4 hours, 12 hours, 24 hours, 2 days, 7 days, 14 days, and 24 days.*

4.5. Cytotoxicity Study

A549 cells have been treated with three different concentrations of empty NC, NC, and FD, the result of this statistic is given in fig. 18. The empty NC X has shown no cytotoxic effect where the cell viability remains around 99% after 72 h. As the concentration of empty NC increases to 4X the cell viability decreases, indicating a toxic effect; due to the increment in the viscosity of cell media, and the decrement of nutrients in cells lowering the cell survival rate. The cytotoxicity gained from empty NC is not desired as it can harm the patient. The cell viability after 72 h for The empty NC 4X reaches 81.66%. The FD and NC show a gradual decrease in cell viability percentage as the drug concentration increase. Comparing FD with NC indicates that the influence of FD within the first 72 hours is better; as the percentage of FD is 100% while the percentage of released drug from NC is around 60%. Comparing the three different

concentrations of NC 50 µg, NC 100 µg, and NC 200 µg, NC100 µg has shown similar results, which are better than NC 50 µg, although the influence of NC 200 µg is the better, we can't ignore the effect of the high concentration of empty NC. So, to gain the desired cytotoxicity with no harm to natural cells, NC 100 µg would be the most efficient dose to treat patients.

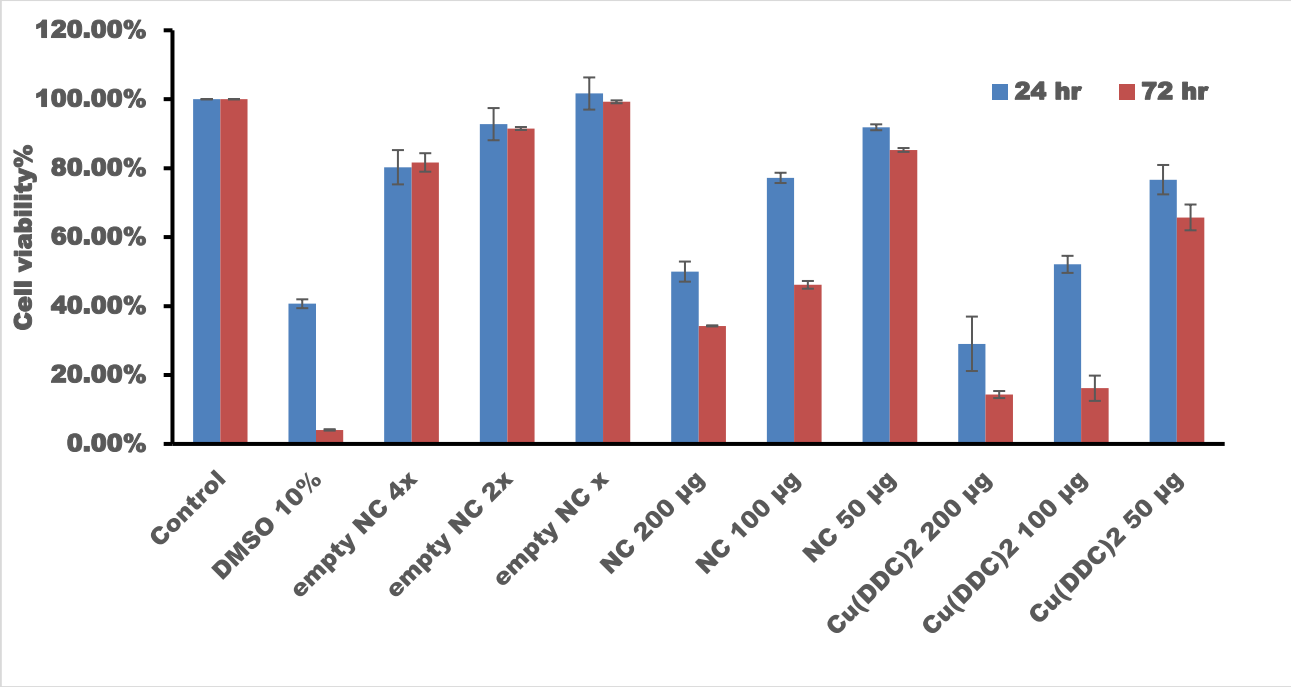

Figure 18. *In vitro cytotoxicity assay of free $Cu(DDC)_2$ and encapsulated $Cu(DDC)_2$ (NC) in A549 cells. Cell viability of A549 cells incubated with free $Cu(DDC)_2$ (FD) and encapsulated $Cu(DDC)_2$ (NC) for 24 hours and 72 hours. Cells viability was examined by MTT assay and expressed as a percentage of untreated controls. Results are expressed as mean ± standard deviation (SD). 4X, 2X, and X denote for empty NC equivalent to NCs containing 200 µg, 100 µg, and 50 µg.*

Conclusion

In this study, we repurposed DSF as an anti-cancer drug, prepared nanoemulsion capsules to carry poorly soluble Cu(DDC)2 in the body and modify the system with PEG and PCL. Out of the three different ratios of PEG:PCL used "25:75, 50:50, 75:25", the ratio that has given us the best particle size with the lowest PDI and good zeta potential was 25:75. So, the rest of the study adopted this ratio, and complete serum stability, drug release, and cytotoxicity study on it. The prepared nanocapsules have shown a notable difference between the stability of the free drug and the capsulated one in FBS, where the %remained concentration of NC after 4 h was higher than the %remained concentration of FD around 5 times more, indicating the enhancement in the circulation lifetime of the drug when capsulated. The observation of the drug release has given an extended-release time, where the release percentage within the first 24 h was around 50%, and in one week it reaches 65.3%, and completing release to reach 97.6% after two weeks, indicating a sustained-release capsule. Finally, the cytotoxicity study of NC has shown an incremental decrease in cell viability with time as the percentage of drug released increases. in consideration of empty nanocapsules cytotoxicity observation, NC 100 mg is the recommended dosage. Although the cytotoxicity effect of FD has the best influence, it cannot be ignored that the use of FD is impossible inside the body as it is poorly soluble in aqueous media, and its serum stability is compromised

References

[1] H. A. Idikio, “Human cancer classification: A systems biology-based model integrating morphology, cancer stem cells, proteomics, and genomics,” *J. Cancer*, vol. 2, no. 1, pp. 107–115, 2011, doi: 10.7150/jca.2.107.

[2] R. Kumar, R. Srivastava, and S. Srivastava, “Detection and Classification of Cancer from Microscopic Biopsy Images Using Clinically Significant and Biologically Interpretable Features,” *J. Med. Eng.*, vol. 2015, pp. 1–14, 2015, doi: 10.1155/2015/457906.

[3] B. J. M. Z. Van Tongeren, L. A. Rook, and A. K. Mantel-teeuwisse, “Priority Medicines for Europe and the World- A Public Health Approach to Innovation,” *Prior. Med. Eur. World*, no. April, pp. 1–55, 2013, [Online]. Available: http://www.who.int/medicines/areas/priority_medicines/BP6_5cancer.pdf%5Cnhttp://www.who.int/medicines/areas/priority_medicines/BP7_2Women.pdf.

[4] Q. Song, S. D. Merajver, and J. Z. Li, “Cancer classification in the genomic era: Five contemporary problems,” *Hum. Genomics*, pp. 1–8, 2015, doi: 10.1186/s40246-015-0049-8.

[5] R. L. Siegel, K. D. Miller, and A. Jemal, “Cancer statistics, 2020,” *CA. Cancer J. Clin.*, vol. 70, no. 1, pp. 7–30, 2020, doi: 10.3322/caac.21590.

[6] W. Mccarthy, “Polymeric Drug Delivery Techniques,” *Aldrich Mater. Sci.*, no. 5, pp. 2–5, 2016.

[7] S. Parveen, R. Misra, and S. K. Sahoo, “Nanoparticles: A boon to drug delivery, therapeutics, diagnostics and imaging,” *Nanomedicine Nanotechnology, Biol. Med.*, vol. 8, no. 2, pp. 147–166, 2012, doi: 10.1016/j.nano.2011.05.016.

[8] O. Kayser, A. Lemke, and N. Hernandez-Trejo, “The Impact of Nanobiotechnology on the Development of New Drug Delivery Systems,” *Curr. Pharm. Biotechnol.*, vol. 6, no. 1, pp. 3–5, 2016, doi: 10.2174/1389201053167158.

[9] S. K. Sahoo and V. Labhasetwar, “Nanotech approaches to drug delivery and imaging,” *Drug Discov. Today*, vol. 8, no. 24, pp. 1112–1120, 2003, doi: 10.1016/S1359-6446(03)02903-9.

[10] E. Blanco, H. Shen, and M. Ferrari, “Principles of nanoparticle design for overcoming biological barriers to drug delivery,” *Nat. Biotechnol.*, vol. 33, no. 9, pp. 941–951, 2015, doi: 10.1038/nbt.3330.

[11] N. S. Oltra, J. Swift, A. Mahmud, K. Rajagopal, S. M. Loverde, and D. E. Discher, “Filomicelles in nanomedicine-from flexible, fragmentable, and ligand-targetable drug carrier designs to combination therapy for brain tumors,” *J. Mater. Chem. B*, vol. 1, no. 39, pp. 5177–5185, 2013, doi: 10.1039/c3tb20431f.

[12] Y. Liu, J. Tan, A. Thomas, D. Ou-Yang, and V. R. Muzykantov, “The shape of things to come: Importance of design in nanotechnology for drug delivery,” *Ther. Deliv.*, vol. 3, no. 2, pp. 181–194, 2012, doi: 10.4155/tde.11.156.

[13] F. Alexis, E. Pridgen, L. K. Molnar, and O. C. Farokhzad, “Factors affecting the clearance and biodistribution of polymeric nanoparticles,” *Mol. Pharm.*, vol. 5, no. 4, pp. 505–515, 2008, doi: 10.1021/mp800051m.

[14] G. Thurston *et al.*, “Cationic liposomes target angiogenic endothelial cells in tumors and chronic inflammation in mice.,” *J. Clin. Invest.*, vol. 101, no. 7, pp. 1401–1413, 1998, doi: 10.1172/jci965.

[15] M. J. Mitchell, M. M. Billingsley, R. M. Haley, M. E. Wechsler, N. A. Peppas, and R. Langer, “Engineering precision nanoparticles for drug delivery,” *Nat. Rev. Drug Discov.*, vol. 20, no. 2, pp. 101–124, 2021, doi: 10.1038/s41573-020-0090-8.

[16] R. Kumar, *Lipid-Based Nanoparticles for Drug-Delivery Systems*. Elsevier Inc., 2019.

[17] M. L. Tebaldi, R. M. Belardi, and S. R. Montoro, *Polymers with Nano-Encapsulated Functional Polymers: Encapsulated Phase Change Materials. Encapsulated Phase Change Materials.* Elsevier Inc., 2016.

[18] W. T. Al-Jamal and K. Kostarelos, “Liposomes: From a clinically established drug delivery system to a nanoparticle platform for theranostic nanomedicine,” *Acc. Chem. Res.*, vol. 44, no. 10, pp. 1094–1104, 2011, doi: 10.1021/ar200105p.

[19] N. Wang, X. Cheng, N. Li, H. Wang, and H. Chen, “Nanocarriers and Their Loading Strategies,” *Adv. Healthc. Mater.*, vol. 8, no. 6, pp. 1–26, 2019, doi: 10.1002/adhm.201801002.

[20] R. Li, Q. Fang, P. Li, C. Zhang, Y. Yuan, and H. Zhuang, “Effects of emulsifier type and post-treatment on stability, curcumin protection, and sterilization ability of nanoemulsions,” *Foods*, vol. 10, no. 1, 2021, doi: 10.3390/foods10010149.

[21] R. Miller, *Emulsifiers: Types and Uses*, 1st ed., no. c. Elsevier Ltd., 2015.

[22] R. I. M. and A. S. Narang, *Pharmaceutical Dosage Forms and Drug Delivery, Third Edition*. 1369.

[23] Y. Zheng, M. Zheng, Z. Ma, B. Xin, R. Guo, and X. Xu, *Sugar Fatty Acid Esters*. AOCS Press, 2015.

[24] E. J. Acosta, J. S. Yuan, and A. S. Bhakta, “The characteristic curvature of ionic surfactants,” *J. Surfactants Deterg.*, vol. 11, no. 2, pp. 145–158, 2008, doi: 10.1007/s11743-008-1065-7.

[25] S. Zarate-Muñoz, F. Texeira De Vasconcelos, K. Myint-Myat, J. Minchom, and E. Acosta, “A Simplified Methodology to Measure the Characteristic Curvature (Cc) of Alkyl Ethoxylate Nonionic Surfactants,” *J. Surfactants Deterg.*, vol. 19, no. 2, pp. 249–263, 2016, doi: 10.1007/s11743-016-1787-x.

[26] M. A. Farooq *et al.*, “Recent advances in the delivery of disulfiram: a critical analysis of promising approaches to improve its pharmacokinetic profile and anticancer efficacy,” *DARU, J. Pharm. Sci.*, vol. 27, no. 2, pp. 853–862, 2019, doi: 10.1007/s40199-019-00308-w.

[27] P. Liu *et al.*, “Liposome encapsulated Disulfiram inhibits NFκB pathway and targets breast cancer stem cells in vitro and in vivo,” *Oncotarget*, vol. 5, no. 17, pp. 7471–7485, 2014, doi: 10.18632/oncotarget.2166.

[28] M. Najlah *et al.*, “Development and characterisation of disulfiram-loaded PLGA nanoparticles

for the treatment of non-small cell lung cancer," *Eur. J. Pharm. Biopharm.*, vol. 112, no. December, pp. 224–233, 2017, doi: 10.1016/j.ejpb.2016.11.032.

[29] W. Q. Ding and S. E. Lind, "Metal ionophores - An emerging class of anticancer drugs," *IUBMB Life*, vol. 61, no. 11, pp. 1013–1018, 2009, doi: 10.1002/iub.253.

[30] Center for Substance Abuse Treatment, "Incorporating Alcohol Pharmacotherapies Into Medical Practice," *Cent. Subst. Abus. Treat.*, vol. 114, p. 126, 2009.

[31] Q. Spillier *et al.*, "Anti-alcohol abuse drug disulfiram inhibits human PHGDH via disruption of its active tetrameric form through a specific cysteine oxidation," *Sci. Rep.*, vol. 9, no. 1, pp. 1–9, 2019, doi: 10.1038/s41598-019-41187-0.

[32] B. A. Johnson and C. Seneviratne, *Alcohol-medical drug interactions*, 1st ed., vol. 125. Elsevier B.V., 2014.

[33] M. Setshedi, J. R. Wands, and S. M. De Monte, "Alcohol Enzyme Polymorphisms," *Oxid. Med. Cell. Longev.*, vol. 3, no. 3, pp. 178–185, 2010.

[34] C. R. Borja Oliveira, "Alcohol-Medication Interactions: The Acetaldehyde Syndrome," *J. Pharmacovigil.*, vol. 02, no. 05, pp. 13–16, 2014, doi: 10.4172/2329-6887.1000145.

[35] R. Rajendram, R. Rajendram, and V. R. Preedy, *Acetaldehyde: A Reactive Metabolite*, vol. 1, no. 2005. Elsevier Inc., 2016.

[36] H. Li, J. Wang, C. Wu, L. Wang, Z. S. Chen, and W. Cui, "The combination of disulfiram and copper for cancer treatment," *Drug Discov. Today*, vol. 25, no. 6, pp. 1099–1108, 2020, doi: 10.1016/j.drudis.2020.04.003.

[37] B. Johansson, "A review of the pharmacokinetics and pharmacodynamics of disulfiram and its metabolites," *Acta Psychiatr. Scand.*, vol. 86, no. 369 S, pp. 15–26, 1992, doi: 10.1111/j.1600-0447.1992.tb03310.x.

[38] C. Wright and R. D. Moore, "Disulfiram treatment of alcoholism," *Am. J. Med.*, vol. 88, no. 6, pp. 647–655, 1990, doi: 10.1016/0002-9343(90)90534-K.

[39] M. Papaioannou, I. Mylonas, R. E. Kast, and A. Brüning, "Disulfiram/copper causes redox-related proteotoxicity and concomitant heat shock response in ovarian cancer cells that is augmented by auranofin-mediated thioredoxin inhibition," *Oncoscience*, vol. 1, no. 1, pp. 21–29, 2014, doi: 10.18632/oncoscience.5.

[40] M. Najlah, "Drug repurposing supported by nanotechnology : a promising strategy to fight cancer chemoresistance "," pp. 9–11, 2021.

[41] M. S. Boguski, K. D. Mandl, and V. P. Sukhatme, "Repurposing with a difference," *Science (80-.).*, vol. 324, no. 5933, pp. 1394–1395, 2009, doi: 10.1126/science.1169920.

[42] T. T. Ashburn and K. B. Thor, "Drug repositioning: Identifying and developing new uses for existing drugs," *Nat. Rev. Drug Discov.*, vol. 3, no. 8, pp. 673–683, 2004, doi: 10.1038/nrd1468.

[43] L. Kaul, R. Süss, A. Zannettino, and K. Richter, "The revival of dithiocarbamates: from pesticides to innovative medical treatments," *iScience*, vol. 24, no. 2, pp. 1–14, 2021, doi:

10.1016/j.isci.2021.102092.

[44] F. Meraz-Torres, S. Plöger, C. Garbe, H. Niessner, and T. Sinnberg, “Disulfiram as a therapeutic agent for metastatic malignant melanoma—old myth or new logos?,” *Cancers (Basel).*, vol. 12, no. 12, pp. 1–20, 2020, doi: 10.3390/cancers12123538.

[45] C. Soave and M. Viola Rhenals, “Repositioning an Old Anti-Alcoholism Drug: Disulfiram as a Selective, Effective and Economical Anticancer Agent,” *J. Dev. Drugs*, vol. 05, no. 02, pp. 3–5, 2016, doi: 10.4172/2329-6631.1000e147.

[46] D. Cen, D. Brayton, B. Shahandeh, F. L. Meyskens, and P. J. Farmer, “Disulfiram facilitates intracellular Cu uptake and induces apoptosis in human melanoma cells,” *J. Med. Chem.*, vol. 47, no. 27, pp. 6914–6920, 2004, doi: 10.1021/jm049568z.

[47] P. Liu *et al.*, “Disulfiram targets cancer stem-like cells and reverses resistance and cross-resistance in acquired paclitaxel-resistant triple-negative breast cancer cells,” *Br. J. Cancer*, vol. 109, no. 7, pp. 1876–1885, 2013, doi: 10.1038/bjc.2013.534.

[48] D. Chen, Q. C. Cui, H. Yang, and Q. P. Dou, “Disulfiram, a clinically used anti-alcoholism drug and copper-binding agent, induces apoptotic cell death in breast cancer cultures and xenografts via inhibition of the proteasome activity,” *Cancer Res.*, vol. 66, no. 21, pp. 10425–10433, 2006, doi: 10.1158/0008-5472.CAN-06-2126.

[49] P. Liu *et al.*, “Cytotoxic effect of disulfiram/copper on human glioblastoma cell lines and ALDH-positive cancer-stem-like cells,” *Br. J. Cancer*, vol. 107, no. 9, pp. 1488–1497, 2012, doi: 10.1038/bjc.2012.442.

[50] M. T. Schweizer *et al.*, “Pharmacodynamic study of disulfiram in men with non-metastatic recurrent prostate cancer,” *Prostate Cancer Prostatic Dis.*, vol. 16, no. 4, pp. 357–361, 2013, doi: 10.1038/pcan.2013.28.

[51] V. Sharma *et al.*, “Disulfiram and its novel derivative sensitize prostate cancer cells to the growth regulatory mechanisms of the cell by re-expressing the epigenetically repressed tumor suppressor—estrogen receptor β,” *Mol. Carcinog.*, vol. 55, no. 11, pp. 1843–1857, 2016, doi: 10.1002/mc.22433.

[52] L. Duan *et al.*, “Inhibitory effect of Disulfiram/copper complex on non-small cell lung cancer cells,” *Biochem. Biophys. Res. Commun.*, vol. 446, no. 4, pp. 1010–1016, 2014, doi: 10.1016/j.bbrc.2014.03.047.

[53] H. Nechushtan *et al.*, “A Phase IIb Trial Assessing the Addition of Disulfiram to Chemotherapy for the Treatment of Metastatic Non-Small Cell Lung Cancer,” *Oncologist*, vol. 20, no. 4, pp. 366–367, 2015, doi: 10.1634/theoncologist.2014-0424.

[54] K. Butcher *et al.*, “Investigation of the key chemical structures involved in the anticancer activity of disulfiram in A549 non-small cell lung cancer cell line,” *BMC Cancer*, vol. 18, no. 1, pp. 1–12, 2018, doi: 10.1186/s12885-018-4617-x.

[55] S. yuan You *et al.*, “Process of immunogenic cell death caused by disulfiram as the anti-colorectal cancer candidate,” *Biochem. Biophys. Res. Commun.*, vol. 513, no. 4, pp. 891–897, 2019, doi: 10.1016/j.bbrc.2019.03.192.

[56] E. Dalla Pozza *et al.*, “Gemcitabine response in pancreatic adenocarcinoma cells is synergistically enhanced by dithiocarbamate derivatives,” *Free Radic. Biol. Med.*, vol. 50, no. 8, pp. 926–933, 2011, doi: 10.1016/j.freeradbiomed.2011.01.001.

[57] S. K. Kim *et al.*, “Reversing the Intractable Nature of Pancreatic Cancer by Selectively Targeting ALDH-High, Therapy-Resistant Cancer Cells,” *PLoS One*, vol. 8, no. 10, pp. 1–11, 2013, doi: 10.1371/journal.pone.0078130.

[58] A. Munshi and R. Ramesh, “Mitogen-Activated Protein Kinases and Their Role in Radiation Response,” *Genes and Cancer*, vol. 4, no. 9–10, pp. 401–408, 2013, doi: 10.1177/1947601913485414.

[59] T. A. Stadheim and G. L. Kucera, “C-Jun N-terminal kinase/stress-activated protein kinase (JNK/SAPK) is required for mitoxantrone- and anisomycin-induced apoptosis in HL-60 cells,” *Leuk. Res.*, vol. 26, no. 1, pp. 55–65, 2002, doi: 10.1016/S0145-2126(01)00099-6.

[60] N. Juretic, J. F. Santibáñez, C. Hurtado, and J. Martínez, “ERK 1,2 and p38 pathways are involved in the proliferative stimuli mediated by urokinase in osteoblastic SaOS-2 cell line,” *J. Cell. Biochem.*, vol. 83, no. 1, pp. 92–98, 2001, doi: 10.1002/jcb.1211.

[61] Y. Wang *et al.*, “Cardiac muscle cell hypertrophy and apoptosis induced by distinct members of the p38 mitogen-activated protein kinase family,” *J. Biol. Chem.*, vol. 273, no. 4, pp. 2161–2168, 1998, doi: 10.1074/jbc.273.4.2161.

[62] H. K. Koul, M. Pal, and S. Koul, “Role of p38 MAP Kinase Signal Transduction in Solid Tumors,” *Genes and Cancer*, vol. 4, no. 9–10, pp. 342–359, 2013, doi: 10.1177/1947601913507951.

[63] J. Zha *et al.*, “Disulfiram targeting lymphoid malignant cell lines via ROS-JNK activation as well as Nrf2 and NF-kB pathway inhibition,” *J. Transl. Med.*, vol. 12, no. 1, pp. 1–9, 2014, doi: 10.1186/1479-5876-12-163.

[64] T. Chiba *et al.*, “Disulfiram eradicates tumor-initiating hepatocellular carcinoma cells in ROS-p38 MAPK pathway-dependent and -independent manners,” *PLoS One*, vol. 9, no. 1, pp. 1–11, 2014, doi: 10.1371/journal.pone.0084807.

[65] J. Zhang *et al.*, “The anti-alcohol dependency drug disulfiram inhibits the viability and progression of gastric cancer cells by regulating the Wnt and NF-κB pathways,” *J. Int. Med. Res.*, vol. 48, no. 6, 2020, doi: 10.1177/0300060520925996.

[66] X. Zhang, S. Linder, and M. Bazzaro, “2020_cancers_Drug Development Targeting the Ubiquitin–Proteasome System (UPS) for the Treatment of Human Cancers.pdf,” pp. 1–34, 2020.

[67] B. Cvek, “Targeting Malignancies with Disulfiram (Antabuse): Multidrug Resistance, Angiogenesis, and Proteasome,” *Curr. Cancer Drug Targets*, vol. 11, no. 3, pp. 332–337, 2011, doi: 10.2174/156800911794519806.

[68] T. W. Loo and D. M. Clarke, “Blockage of drug resistance in vitro by disulfiram, a drug used to treat alcoholism,” *J. Natl. Cancer Inst.*, vol. 92, no. 11, pp. 898–902, 2000, doi: 10.1093/jnci/92.11.898.

[69] T. Sun *et al.*, “Erratum: Induction of immunogenic cell death in radiation-resistant breast cancer stem cells by repurposing anti-alcoholism drug disulfiram (Cell Communication and Signaling (2020) 18 (36) DOI: 10.1186/s12964-019-0507-3),” *Cell Commun. Signal.*, vol. 18, no. 1, pp. 1–14, 2020, doi: 10.1186/s12964-020-00567-0.

[70] R. Wang *et al.*, “The evolving role of disulfiram in radiobiology and the treatment of breast cancer,” *Onco. Targets. Ther.*, vol. 13, pp. 10441–10446, 2020, doi: 10.2147/OTT.S271532.

[71] M. A. Farooq *et al.*, “Recent advances in the delivery of disulfiram: a critical analysis of promising approaches to improve its pharmacokinetic profile and anticancer efficacy,” *DARU, J. Pharm. Sci.*, vol. 27, no. 2, pp. 853–862, 2019, doi: 10.1007/s40199-019-00308-w.

[72] Z. Skrott *et al.*, “Disulfiram’s anti-cancer activity reflects targeting NPL4, not inhibition of aldehyde dehydrogenase,” *Oncogene*, vol. 38, no. 40, pp. 6711–6722, 2019, doi: 10.1038/s41388-019-0915-2.

[73] K. R. Frazier, J. A. Moore, and T. E. Long, “Antibacterial activity of disulfiram and its metabolites,” *J. Appl. Microbiol.*, vol. 126, no. 1, pp. 79–86, 2019, doi: 10.1111/jam.14094.

[74] A. Messerschmidt, “Copper metalloenzymes,” *Compr. Nat. Prod. II Chem. Biol.*, vol. 8, pp. 489–545, 2010, doi: 10.1016/b978-008045382-8.00180-5.

[75] T. Brown, “Deisign thinking,” *Harv. Bus. Rev.*, vol. 86, no. 6, pp. 84–92, 2008, doi: 10.1002/med.

[76] C. Santini, M. Pellei, V. Gandin, M. Porchia, F. Tisato, and C. Marzano, “Advances in copper complexes as anticancer agents,” *Chem. Rev.*, vol. 114, no. 1, pp. 815–862, 2014, doi: 10.1021/cr400135x.

[77] H. Irving and R. J. P. Williams, “Order of stability of metal complexes,” *Nature*, vol. 162, no. 4123, pp. 746–747, 1948, doi: 10.1038/162746a0.

[78] C. G. Fraga, “Relevance, essentiality and toxicity of trace elements in human health,” *Mol. Aspects Med.*, vol. 26, no. 4-5 SPEC. ISS., pp. 235–244, 2005, doi: 10.1016/j.mam.2005.07.013.

[79] D. J. Kuhn *et al.*, “The Prevention Program, Barbara Ann Karmanos Cancer Institute, and Department of Pathology, School of Medicine, Wayne State University, Detroit, Michigan, USA, 2 Department of Chemistry, College of Arts and Sciences, University of South Florida, Tampa, Fl,” no. 1, pp. 2605–2617, 2004.

[80] J. F. Collins, *Copper: Basic Physiological and Nutritional Aspects*. Elsevier Inc., 2016.

[81] J. H. Menkes, “Menkes disease and Wilson disease: Two sides of the same copper coin: Part I: Menkes disease,” *Eur. J. Paediatr. Neurol.*, vol. 3, no. 4, pp. 147–158, 1999, doi: 10.1016/S1090-3798(99)90048-X.

[82] S. G. Kaler, *Inborn errors of copper metabolism*, 1st ed., vol. 113. Elsevier B.V., 2013.

[83] M. Broadley, P. Brown, I. Cakmak, Z. Rengel, and F. Zhao, *Function of Nutrients: Micronutrients*. 2011.

[84] S. Wei, L. Gao, C. Wu, F. Qin, and J. Yuan, “Role of the lysyl oxidase family in organ

development (Review),” *Exp. Ther. Med.*, vol. 20, no. 1, pp. 163–172, 2020, doi: 10.3892/etm.2020.8731.

[85] L. I. Smith-Mungo and H. M. Kagan, “Lysyl oxidase: Properties, regulation and multiple functions in biology,” *Matrix Biol.*, vol. 16, no. 7, pp. 387–398, 1998, doi: 10.1016/S0945-053X(98)90012-9.

[86] B. J. Brazeau, B. J. Johnson, and C. M. Wilmot, “Copper-containing amine oxidases. Biogenesis and catalysis; a structural perspective,” *Arch. Biochem. Biophys.*, vol. 428, no. 1, pp. 22–31, 2004, doi: 10.1016/j.abb.2004.03.034.

[87] R. Tofalo, G. Perpetuini, M. Schirone, and G. Suzzi, *Biogenic Amines: Toxicology and Health Effect*, 1st ed. Elsevier Ltd., 2015.

[88] C. Giacomelli *et al.*, “Copper (II) ions modulate Angiogenin activity in human endothelial cells,” *Int. J. Biochem. Cell Biol.*, vol. 60, pp. 185–196, 2015, doi: 10.1016/j.biocel.2015.01.005.

[89] E. Urso and M. Maffia, “Behind the Link between Copper and Angiogenesis: Established Mechanisms and an Overview on the Role of Vascular Copper Transport Systems,” *J. Vasc. Res.*, vol. 52, no. 3, pp. 172–196, 2015, doi: 10.1159/000438485.

[90] S. B. Nayak, V. R. Bhat, D. Upadhyay, and S. L. Udupa, “Copper and ceruloplasmin status in serum of prostate and colon cancer patients,” *Indian J. Physiol. Pharmacol.*, vol. 47, no. 1, pp. 108–110, 2003.

[91] K. G. Daniel, P. Gupta, R. H. Harbach, W. C. Guida, and Q. P. Dou, “Organic copper complexes as a new class of proteasome inhibitors and apoptosis inducers in human cancer cells,” *Biochem. Pharmacol.*, vol. 67, no. 6, pp. 1139–1151, 2004, doi: 10.1016/j.bcp.2003.10.031.

[92] A. Scanni, L. Licciardello, M. Trovato, M. Tomirotti, and M. Biraghi, “Serum copper and ceruloplasmin levels in patients with neoplasias localized in the stomach, large intestine or lung,” *Tumori*, vol. 63, no. 2, pp. 175–180, 1977, doi: 10.1177/030089167706300208.

[93] M. Zowczak, M. Iskra, L. Torliński, and S. Cofta, “Analysis of serum copper zinc concentrations in cancer patients,” *Biol. Trace Elem. Res.*, vol. 82, no. 1–3, pp. 1–8, 2001, doi: 10.1385/BTER:82:1-3:001.

[94] L. Turecký, P. Kalina, E. Uhlíková, S. Námerová, and J. Križko, “Serum ceruloplasmin and copper levels in patients with primary brain tumors,” *Klin. Wochenschr.*, vol. 62, no. 4, pp. 187–189, 1984, doi: 10.1007/BF01731643.

[95] A. Chan, F. Wong, and M. Arumanayagam, “Serum ultrafiltrable copper, total copper and caeruloplasmin concentrations in gynaecological carcinomas,” *Ann. Clin. Biochem.*, vol. 30, no. 6, pp. 545–549, 1993, doi: 10.1177/000456329303000603.

[96] S. Brem, “Angiogenesis and cancer control: From concept to therapeutic trial,” *Cancer Control*, vol. 6, no. 5, pp. 436–458, 1999, doi: 10.1177/107327489900600502.

[97] G. J. Brewer, “Copper control as an antiangiogenic anticancer therapy: Lessons from treating Wilson’s disease,” *Exp. Biol. Med.*, vol. 226, no. 7, pp. 665–673, 2001, doi: 10.1177/153537020222600712.

[98] T. Theophanides and J. Anastassopoulou, “Copper and carcinogenesis,” *Crit. Rev. Oncol. Hematol.*, vol. 42, no. 1, pp. 57–64, 2002, doi: 10.1016/S1040-8428(02)00007-0.

[99] Q. Pan *et al.*, “Copper deficiency induced by tetrathiomolybdate suppresses tumor growth and angiogenesis,” *Cancer Res.*, vol. 62, no. 17, pp. 4854–4859, 2002.

[100] J. Yoshii *et al.*, “The copper-chelating agent, trientine, suppresses tumor development and angiogenesis in the murine hepatocellular carcinoma cells,” *Int. J. Cancer*, vol. 94, no. 6, pp. 768–773, 2001, doi: 10.1002/ijc.1537.

[101] S. S. Brem, D. Zagzag, A. M. C. Tsanaclis, S. Gately, M. P. Elkouby, and S. E. Brien, “Inhibition of angiogenesis and tumor growth in the brain. Suppression of endothelial cell turnover by penicillamine and the depletion of copper an angiogenic cofactor,” *Am. J. Pathol.*, vol. 137, no. 5, pp. 1121–1142, 1990.

[102] J. B. Sunwoo *et al.*, “Novel proteasome inhibitor PS-341 inhibits activation of nuclear factor-κB, cell survival, tumor growth, and angiogenesis in squamous cell carcinoma,” *Clin. Cancer Res.*, vol. 7, no. 5, pp. 1419–1428, 2001.

[103] T. Oikawa *et al.*, “The proteasome is involved in angiogenesis,” *Biochem. Biophys. Res. Commun.*, vol. 246, no. 1, pp. 243–248, 1998, doi: 10.1006/bbrc.1998.8604.

[104] J. Adams, “Potential for proteasome inhibition in the treatment of cancer,” *Drug Discov. Today*, vol. 8, no. 7, pp. 307–315, 2003, doi: 10.1016/S1359-6446(03)02647-3.

[105] Q. P. Dou and B. Li, “Proteasome inhibitors as potential novel anticancer agents,” *Drug Resist. Updat.*, vol. 2, no. 4, pp. 215–223, 1999, doi: 10.1054/drup.1999.0095.

[106] J. B. Almond and G. M. Cohen, “The proteasome: A target novel for cancer chemotherapy,” *Leukemia*, vol. 16, no. 4, pp. 433–443, 2002, doi: 10.1038/sj.leu.2402417.

[107] A. L. Goldberg, “PEIPRSPECTIVES Functions of the Proteasome : The Lysis at the End of the Tunnel the Cradle to the Grave : Ring Complexes in the Life of a Protein,” vol. 268, no. 12, pp. 12–13, 2000.

[108] H. Fasehee *et al.*, “Delivery of disulfiram into breast cancer cells using folate-receptor-targeted PLGA-PEG nanoparticles: In vitro and in vivo investigations,” *J. Nanobiotechnology*, vol. 14, no. 1, pp. 1–18, 2016, doi: 10.1186/s12951-016-0183-z.

[109] A. Das, P. K. Mandal, F. J. Lovas, C. Medcraft, N. R. Walker, and E. Arunan, “The H2S Dimer is Hydrogen-Bonded: Direct Confirmation from Microwave Spectroscopy,” *Angew. Chemie - Int. Ed.*, vol. 57, no. 46, pp. 15199–15203, 2018, doi: 10.1002/anie.201808162.

[110] M. Wehbe, “Copper-Based Therapeutics: Creating a Formulation Platform To Facilitate Development of an Emerging Drug Class,” no. October, 2012.

[111] M. Viola-Rhenals, K. R. Patel, L. Jaimes-Santamaria, G. Wu, J. Liu, and Q. P. Dou, “Recent Advances in Antabuse (Disulfiram): The Importance of its Metal-binding Ability to its Anticancer Activity,” *Curr. Med. Chem.*, vol. 25, no. 4, pp. 506–524, 2018, doi: 10.2174/0929867324666171023161121.

[112] A. Calderon-Aparicio, M. Strasberg-Rieber, and M. Rieber, “Disulfiram anti-cancer efficacy without copper overload is enhanced by extracellular H2O2 generation: Antagonism by tetrathiomolybdate,” *Oncotarget*, vol. 6, no. 30, pp. 29771–29781, 2015, doi: 10.18632/oncotarget.4833.

[113] N. C. Yip *et al.*, “Disulfiram modulated ROS-MAPK and NFB pathways and targeted breast cancer cells with cancer stem cell-like properties,” *Br. J. Cancer*, vol. 104, no. 10, pp. 1564–1574, 2011, doi: 10.1038/bjc.2011.126.

[114] C. Rae, M. Tesson, J. W. Babich, M. Boyd, A. Sorensen, and R. J. Mairs, “The role of copper in disulfiram-induced toxicity and radiosensitization of cancer cells,” *J. Nucl. Med.*, vol. 54, no. 6, pp. 953–960, 2013, doi: 10.2967/jnumed.112.113324.

[115] P. Liu *et al.*, “Cytotoxic effect of disulfiram/copper on human glioblastoma cell lines and ALDH-positive cancer-stem-like cells,” *Br. J. Cancer*, vol. 107, no. 9, pp. 1488–1497, 2012, doi: 10.1038/bjc.2012.442.

[116] P. Zhao, X. Tang, and Y. Huang, “Teaching new tricks to old dogs: A review of drug repositioning of disulfiram for cancer nanomedicine,” *View*, no. January, p. 20200127, 2021, doi: 10.1002/viw.20200127.

[117] A. M. L. S. M. Christopher, *HHS Public Access*, vol. 176, no. 1. 2016.

[118] S. Guo and L. Huang, “Nanoparticles containing insoluble drug for cancer therapy,” *Biotechnol. Adv.*, vol. 32, no. 4, pp. 778–788, 2014, doi: 10.1016/j.biotechadv.2013.10.002.

[119] R. C. Feitosa, D. C. Geraldes, V. L. Beraldo-De-Araújo, J. S. R. Costa, and L. Oliveira-Nascimento, “Pharmacokinetic aspects of nanoparticle-in-matrix drug delivery systems for oral/buccal delivery,” *Front. Pharmacol.*, vol. 10, no. SEP, 2019, doi: 10.3389/fphar.2019.01057.

[120] D. Chenthamara *et al.*, “Therapeutic efficacy of nanoparticles and routes of administration,” *Biomater. Res.*, vol. 23, no. 1, pp. 1–29, 2019, doi: 10.1186/s40824-019-0166-x.

[121] X. Li *et al.*, “Therapeutic efficacy of nanoparticles and routes of administration,” *Biomater. Res.*, vol. 23, no. 1, pp. 654–663, 2019, doi: 10.1016/j.biotechadv.2013.10.002.

[122] P. Zhao, X. Tang, and Y. Huang, “Teaching new tricks to old dogs: A review of drug repositioning of disulfiram for cancer nanomedicine,” *View*, no. December 2020, p. 20200127, 2021, doi: 10.1002/viw.20200127.

[123] M. Chakravarty and A. Vora, *Delivery Applications*. 2020.

[124] R. Wen, A. C. Umeano, P. Chen, and A. A. Farooqi, “Polymer-based drug delivery systems for cancer,” *Crit. Rev. Ther. Drug Carrier Syst.*, vol. 35, no. 6, pp. 521–554, 2018, doi: 10.1615/CritRevTherDrugCarrierSyst.2018021124.

[125] T. Aminabhavi, R. Kulkarni, and A. Kulkarni, “Column: Polymers in Drug Delivery,” *Polym. News*, vol. 29, no. 7, pp. 214–218, 2004, doi: 10.1080/003239104909811164.

[126] X. Guo, L. Wang, X. Wei, and S. Zhou, “Polymer-based drug delivery systems for cancer treatment,” *J. Polym. Sci. Part A Polym. Chem.*, vol. 54, no. 22, pp. 3525–3550, 2016, doi:

10.1002/pola.28252.

[127] G. Giammona and E. F. Craparo, “Polymer-based systems for controlled release and targeting of drugs,” *Polymers (Basel).*, vol. 11, no. 12, pp. 10–12, 2019, doi: 10.3390/polym11122066.

[128] S. Scioli Montoto, G. Muraca, and M. E. Ruiz, “Solid Lipid Nanoparticles for Drug Delivery: Pharmacological and Biopharmaceutical Aspects,” *Front. Mol. Biosci.*, vol. 7, no. October, pp. 1–24, 2020, doi: 10.3389/fmolb.2020.587997.

[129] Y. Duan *et al.*, “A brief review on solid lipid nanoparticles: Part and parcel of contemporary drug delivery systems,” *RSC Adv.*, vol. 10, no. 45, pp. 26777–26791, 2020, doi: 10.1039/d0ra03491f.

[130] M. Harms and C. C. Müller-Goymann, “Solid lipid nanoparticles for drug delivery,” *J. Drug Deliv. Sci. Technol.*, vol. 21, no. 1, pp. 89–99, 2011, doi: 10.1016/S1773-2247(11)50008-5.

[131] A. Deshpande, M. Mohamed, S. B. Daftardar, M. Patel, S. H. S. Boddu, and J. Nesamony, *Solid Lipid Nanoparticles in Drug Delivery: Opportunities and Challenges*. Elsevier, 2017.

[132] A. A. Attama, M. A. Momoh, and P. F. Builders, “Chapter 5-Lipid nanoparticulate drug delivery systems: a revolution in dosage form design and development,” *Recent Adv. Nov. Drug Carr. Syst.*, pp. 107–140, 2012, [Online]. Available: http://www.intechopen.com/books/recent-advances-in-novel-drug-carrier-systems/lipid-nanoparticulate-drug-delivery-systems-a-revolution-in-dosage-form-design-and-development.

[133] V. P. Torchilin, “Recent advances with liposomes as pharmaceutical carriers,” *Nat. Rev. Drug Discov.*, vol. 4, no. 2, pp. 145–160, 2005, doi: 10.1038/nrd1632.

[134] A. T.S, K. T. Shalumon, and J.-P. Chen, “Applications of Magnetic Liposomes in Cancer Therapies,” *Curr. Pharm. Des.*, vol. 25, no. 13, pp. 1490–1504, 2019, doi: 10.2174/1389203720666190521114936.

[135] N. Düzgüneş, J. Piskorz, P. Skupin-Mrugalska, T. Goslinski, J. Mielcarek, and K. Konopka, “Photodynamic therapy of cancer with liposomal photosensitizers,” *Ther. Deliv.*, vol. 9, no. 11, pp. 823–832, 2018, doi: 10.4155/tde-2018-0050.

[136] Y. Yang *et al.*, “Photodynamic Therapy with Liposomes Encapsulating Photosensitizers with Aggregation-Induced Emission,” *Nano Lett.*, vol. 19, no. 3, pp. 1821–1826, 2019, doi: 10.1021/acs.nanolett.8b04875.

[137] X. Zhang *et al.*, “Liposomes equipped with cell penetrating peptide BR2 enhances chemotherapeutic effects of cantharidin against hepatocellular carcinoma,” *Drug Deliv.*, vol. 24, no. 1, pp. 986–998, 2017, doi: 10.1080/10717544.2017.1340361.

[138] B. A. Khaw, J. DaSilva, I. Vural, J. Narula, and V. P. Torchilin, “Intracytoplasmic gene delivery for in vitro transfection with cytoskeleton-specific immunoliposomes,” *J. Control. Release*, vol. 75, no. 1–2, pp. 199–210, 2001, doi: 10.1016/S0168-3659(01)00364-9.

[139] P. Pandey and M. Dahiya, “A Brief Review on Inorganic Nanoparticles,” *J. Crit. Rev.*, vol. 3, no. 3, pp. 18–26, 2016.

[140] Y. Ghosn *et al.*, “Inorganic Nanoparticles as Drug Delivery Systems and Their Potential Role in the Treatment of Chronic Myelogenous Leukaemia,” *Technol. Cancer Res. Treat.*, vol. 18, pp. 1–12, 2019, doi: 10.1177/1533033819853241.

[141] W. Paul and C. P. Sharma, *Inorganic nanoparticles for targeted drug delivery*. Elsevier Ltd, 2019.

[142] J. A. R. Jonathan Posner and Bradley S. Peterson, “NIH Public Access,” *Bone*, vol. 23, no. 1, pp. 1–7, 2008, doi: 10.1016/j.cocis.2014.03.004.Inorganic.

[143] C. P. Sharma, “Biointegration of medical implant materials: Science and design,” *Biointegration Med. Implant Mater. Sci. Des.*, pp. 1–412, 2010, doi: 10.1533/9781845699802.

[144] P. P. Pednekar, S. C. Godiyal, K. R. Jadhav, and V. J. Kadam, *Chapter 23 - Mesoporous silica nanoparticles: a promising multifunctional drug delivery system*. Elsevier Inc., 2017.

[145] H. A. Santos, L. M. Bimbo, L. Peltonen, and J. Hirvonen, *Inorganic Nanoparticles in Targeted Drug Delivery and Imaging*. 2015.

[146] N. Bydlinski, “www.proteomics-journal.com Page 1 Proteomics,” *Proteomics*, pp. 1–25, 2013, doi: 10.1002/jssc.201200569.

[147] W. Chen, W. Yang, P. Chen, Y. Huang, and F. Li, “Disulfiram Copper Nanoparticles Prepared with a Stabilized Metal Ion Ligand Complex Method for Treating Drug-Resistant Prostate Cancers,” *ACS Appl. Mater. Interfaces*, vol. 10, no. 48, pp. 41118–41128, 2018, doi: 10.1021/acsami.8b14940.

[148] P. Banerjee, T. Geng, A. Mahanty, T. Li, L. Zong, and B. Wang, “Integrating the drug, disulfiram into the vitamin E-TPGS-modified PEGylated nanostructured lipid carriers to synergize its repurposing for anti-cancer therapy of solid tumors,” *Int. J. Pharm.*, vol. 557, no. January, pp. 374–389, 2019, doi: 10.1016/j.ijpharm.2018.12.051.

[149] I. S. Mohammad, W. He, and L. Yin, “A Smart Paclitaxel-Disulfiram Nanococrystals for Efficient MDR Reversal and Enhanced Apoptosis,” *Pharm. Res.*, vol. 35, no. 4, 2018, doi: 10.1007/s11095-018-2370-0.

[150] J. K. Patra *et al.*, “Nano based drug delivery systems: Recent developments and future prospects 10 Technology 1007 Nanotechnology 03 Chemical Sciences 0306 Physical Chemistry (incl. Structural) 03 Chemical Sciences 0303 Macromolecular and Materials Chemistry 11 Medical and He,” *J. Nanobiotechnology*, vol. 16, no. 1, pp. 1–33, 2018, doi: 10.1186/s12951-018-0392-8.

[151] P. Decuzzi *et al.*, “Roadmap on nanomedicine,” *Nanotechnology*, vol. 32, no. 1, 2021, doi: 10.1088/1361-6528/abaadb.

[152] Y. Yao *et al.*, “Nanoparticle-Based Drug Delivery in Cancer Therapy and Its Role in Overcoming Drug Resistance,” *Front. Mol. Biosci.*, vol. 7, no. August, pp. 1–14, 2020, doi: 10.3389/fmolb.2020.00193.

[153] B. He, X. Sui, B. Yu, S. Wang, Y. Shen, and H. Cong, “Recent advances in drug delivery systems for enhancing drug penetration into tumors,” *Drug Deliv.*, vol. 27, no. 1, pp. 1474–1490, 2020,

doi: 10.1080/10717544.2020.1831106.

[154] S. Rajesh and J. W. L. Jr., “Nanoparticle-based targeted drug delivery,” *Exp. Mol. Pathol.*, vol. 86, no. 3, pp. 215–223, 2000, doi: 10.1016/j.yexmp.2008.12.004.Nanoparticle-based.

[155] J. Fang, W. Islam, and H. Maeda, “Exploiting the dynamics of the EPR effect and strategies to improve the therapeutic effects of nanomedicines by using EPR effect enhancers,” *Adv. Drug Deliv. Rev.*, vol. 157, pp. 142–160, 2020, doi: 10.1016/j.addr.2020.06.005.

[156] S. A. A. Rizvi and A. M. Saleh, “Applications of nanoparticle systems in drug delivery technology,” *Saudi Pharm. J.*, vol. 26, no. 1, pp. 64–70, 2018, doi: 10.1016/j.jsps.2017.10.012.

[157] M. Zhang, Y. Du, S. Wang, and B. Chen, “A review of biomimetic nanoparticle drug delivery systems based on cell membranes,” *Drug Des. Devel. Ther.*, vol. 14, pp. 5495–5503, 2020, doi: 10.2147/DDDT.S282368.

[158] D. N. Kapoor, A. Bhatia, R. Kaur, R. Sharma, G. Kaur, and S. Dhawan, “PLGA: A unique polymer for drug delivery,” *Ther. Deliv.*, vol. 6, no. 1, pp. 41–58, 2015, doi: 10.4155/tde.14.91.

[159] Z. Wang *et al.*, *Poly lactic-co-glycolic acid controlled delivery of disulfiram to target liver cancer stem-like cells*, vol. 13, no. 2. Elsevier B.V., 2017.

[160] H. Fasehee, A. Ghavamzadeh, K. Alimoghaddam, S. Ghaffari, and S. Faghihi, “A Comparative Cytotoxic Evaluation of Disulfiram,” *Int. J. Hematol. Stem Cell Res.*, vol. 11, no. 2, pp. 102–107, 2017.

[161] H. Fasehee, G. Zarrinrad, and S. Mohammad, “The inhibitory effect of disul fi ram encapsulated PLGA NPs on tumor growth : Different administration routes,” *Mater. Sci. Eng. C*, vol. 63, pp. 587–595, 2016, doi: 10.1016/j.msec.2016.03.023.

[162] M. Hoda, S. Pajaniradje, G. Shakya, K. Mohankumar, and R. Rajagopalan, “Anti-proliferative and apoptosis-triggering potential of disulfiram and disulfiram-loaded polysorbate 80-stabilized PLGA nanoparticles on hepatocellular carcinoma Hep3B cell line,” *Nanomedicine Nanotechnology, Biol. Med.*, vol. 12, no. 6, pp. 1641–1650, 2016, doi: 10.1016/j.nano.2016.02.013.

[163] H. He, E. Markoutsa, J. Li, and P. Xu, “Repurposing Disulfiram for Cancer Therapy via Targeted Nanotechnology through Enhanced Tumor Mass Penetration and Disassembly,” *Acta Biomater.*, 2017, doi: 10.1016/j.actbio.2017.12.023.

[164] X. Zhuo *et al.*, “Journal of Colloid and Interface Science Disulfiram-loaded mixed nanoparticles with high drug-loading and plasma stability by reducing the core crystallinity for intravenous delivery,” *J. Colloid Interface Sci.*, vol. 529, pp. 34–43, 2018, doi: 10.1016/j.jcis.2018.05.057.

[165] S. Loading *et al.*, “Stable Loading and Delivery of Disulfiram with mPEG-PLGA/PCL Mixed Nanoparticles for Tumor Therapy Wantong,” 2015, doi: 10.1016/j.nano.2015.10.022.

[166] X. Tao *et al.*, “Synergistic breast tumor cell killing achieved by intracellular co-delivery of doxorubicin and disulfiram: Via core-shell-corona nanoparticles,” *Biomater. Sci.*, vol. 6, no. 7, pp. 1869–1881, 2018, doi: 10.1039/c8bm00271a.

[167] W. Song *et al.*, “Combining disul fi ram and poly (L -glutamic acid) -cisplatin conjugates for combating cisplatin resistance,” *J. Control. Release*, pp. 2–10, 2016, doi: 10.1016/j.jconrel.2016.02.039.

[168] H. R. Madala, S. R. Punganuru, F. Ali-Osman, R. Zhang, and K. S. Srivenugopal, “Brain- and brain tumor-penetrating disulfiram nanoparticles: Sequence of cytotoxic events and efficacy in human glioma cell lines and intracranial xenografts,” *Oncotarget*, vol. 9, no. 3, pp. 3459–3482, 2018, doi: 10.18632/oncotarget.23320.

[169] Y. Zhong *et al.*, “N-Oxide polymer-cupric ion nanogels potentiate disulfiram for cancer therapy,” *Biomater. Sci.*, vol. 8, no. 6, pp. 1726–1733, 2020, doi: 10.1039/c9bm01841g.

[170] D. Press, “Micelles for the Co-Delivery of Paclitaxel / Disulfiram and Overcoming Multidrug Resistance in Cancer,” pp. 8631–8647, 2017.

[171] T.-C. P. Micelles and C. Therapy, “Smart pH-Sensitive and Temporal- Controlled Polymeric Micelles for E ff ective Combination Therapy of,” *ACS Nano*, vol. 7, no. 7, pp. 5858–5869, 2013.

[172] X. Peng *et al.*, “Highly Stable, Coordinated Polymeric Nanoparticles Loading Copper(II) Diethyldithiocarbamate for Combinational Chemo/Chemodynamic Therapy of Cancer,” *Biomacromolecules*, vol. 20, no. 6, pp. 2372–2383, 2019, doi: 10.1021/acs.biomac.9b00367.

[173] X. Duan, Q. Yin, Z. Zhang, and H. Yu, “Multi-targeted inhibition of tumor growth and lung metastasis by redox- sensitive shell crosslinked micelles loading disulfiram Multi-targeted inhibition of tumor growth and lung metastasis by redox-sensitive shell,” no. June 2015, 2014, doi: 10.1088/0957-4484/25/12/125102.

[174] L. Zhang *et al.*, “A Copper-Mediated Disulfiram-Loaded pH-Triggered PEG-Shedding TAT Peptide-Modified Lipid Nanocapsules for Use in Tumor Therapy,” *ACS Appl. Mater. Interfaces*, vol. 7, no. 45, pp. 25147–25161, 2015, doi: 10.1021/acsami.5b06488.

[175] M. Wehbe *et al.*, “Development and optimization of an injectable formulation of copper diethyldithiocarbamate, an active anticancer agent,” *Int. J. Nanomedicine*, vol. 12, pp. 4129–4146, 2017, doi: 10.2147/IJN.S137347.

[176] L. Zhou *et al.*, “Membrane Loaded Copper Oleate PEGylated Liposome Combined with Disulfiram for Improving Synergistic Antitumor Effect In Vivo,” pp. 1–11, 2018.

[177] M. Najlah, A. S. Suliman, I. Tolaymat, and S. Kurusamy, “Development of Injectable PEGylated Liposome Encapsulating Disulfiram for Colorectal Cancer Treatment,” pp. 1–16, 2019.

[178] Y. Qu *et al.*, “Nose-to-brain delivery of disulfiram nanoemulsion in situ gel formulation for glioblastoma targeting therapy,” *Int. J. Pharm.*, vol. 597, no. December 2020, p. 120250, 2021, doi: 10.1016/j.ijpharm.2021.120250.

[179] H. Chen *et al.*, “Tumor-responsive copper-activated disulfiram for synergetic nanocatalytic tumor therapy,” *Nano Res.*, vol. 14, no. 1, pp. 205–211, 2021, doi: 10.1007/s12274-020-3069-1.

[180] K. Zuhra *et al.*, “Mechanism of cystathionine-β-synthase inhibition by disulfiram: The role of bis(N,N-diethyldithiocarbamate)-copper(II),” *Biochem. Pharmacol.*, vol. 182, no. Ii, p. 114267,

2020, doi: 10.1016/j.bcp.2020.114267.

[181] I. S. Mohammad, C. Teng, B. Chaurasiya, L. Yin, C. Wu, and W. He, “Drug-delivering-drug approach-based codelivery of paclitaxel and disulfiram for treating multidrug-resistant cancer,” *Int. J. Pharm.*, vol. 557, no. December 2018, pp. 304–313, 2019, doi: 10.1016/j.ijpharm.2018.12.067.

[182] W. Wu *et al.*, “Enhanced Tumor-Specific Disulfiram Chemotherapy by in Situ Cu2+ Chelation-Initiated Nontoxicity-to-Toxicity Transition,” *J. Am. Chem. Soc.*, vol. 141, no. 29, pp. 11531–11539, 2019, doi: 10.1021/jacs.9b03503.

[183] W. Wu, L. Yu, Y. Pu, H. Yao, Y. Chen, and J. Shi, “Copper-Enriched Prussian Blue Nanomedicine for In Situ Disulfiram Toxification and Photothermal Antitumor Amplification,” *Adv. Mater.*, vol. 32, no. 17, pp. 1–12, 2020, doi: 10.1002/adma.202000542.

[184] B. Karen, A. Seabolt, and C. Editor, “Learning About Lecithin,” vol. 23, no. 3, pp. 4–5, 2013.

[185] N. Ng *et al.*, “Lipid digestion of oil-in-water emulsions stabilized with low molecular weight surfactants,” *Food Funct.*, vol. 10, no. 12, pp. 8195–8207, 2019, doi: 10.1039/c9fo02210d.

[186] S. Gittings, “Development of Biorelevant Simulated Salivary Fluids for Application in Dissolution Testing Thesis submitted to the University of,” *PhD Thesis*, vol. University, no. September, p. 37, 2017, [Online]. Available: http://eprints.nottingham.ac.uk/39862/1/Thesis FINAL version for%0A submission_Sally Gittings.pdf.

[187] S. Moffatt, “Nanoparticle PEGylation for Cancer Therapy,” *MOJ Proteomics Bioinforma.*, vol. 2, no. 1, pp. 9–11, 2015, doi: 10.15406/mojpb.2015.02.00037.

[188] R. Z. Xiao, Z. W. Zeng, G. L. Zhou, J. J. Wang, F. Z. Li, and A. M. Wang, “Recent advances in PEG-PLA block copolymer nanoparticles,” *Int. J. Nanomedicine*, vol. 5, no. 1, pp. 1057–1065, 2010, doi: 10.2147/IJN.S14912.

[189] A. S. Suliman *et al.*, “Cyclodextrin diethyldithiocarbamate copper ii inclusion complexes: A promising chemotherapeutic delivery system against chemoresistant triple negative breast cancer cell lines,” *Pharmaceutics*, vol. 13, no. 1, pp. 1–12, 2021, doi: 10.3390/pharmaceutics13010084.

[190] S. Majid and K. S. Ahmad, “Optical and morphological properties of environmentally benign Cu-Tin sulphide thin films grown by physical vapor deposition technique,” *Mater. Res. Express*, vol. 6, no. 3, 2019, doi: 10.1088/2053-1591/aaf454.

[191] A. S. Suliman *et al.*, “Supplementary Materials : Cyclodextrin Diethyldithiocarba- mate Copper II Inclusion Complexes : A Promising Chemother- apeutic Delivery System against Chemoresistant Triple Nega- tive Breast Cancer Cell Lines,” pp. 2–5, 2021.

الملخّص

أصبح إعادة استخدام العقاقير المخصصة لمرض ما لعلاج أمراض اخرى طريقة فعالة لعلاج الأمراض؛ حيث أنها تعتمد على استخدام مركبات مدروسة الفعالية والسمية على جسم الانسان مسبقاً، مقللاً مخاطر استخدامها. الدِّيسلفيرام *Disulfiram (DSF)*، دواء معروف لعلاج إدمان الكحول بموافقة إدارة الغذاء والدواء (FDA) منذ عام 1951، وجد أن له تأثير مضاد للسرطان عند اتحاده مع أيونات النحاس الثنائية مشكلاً مركب (*bis (N, N-diethyldithiocarbamate) Cu (II)*) ($Cu(DDC)_2$). تتمثل القيود لاستخدام هذا المركب في قابلية ذوبانه الضعيفة في الأوساط المائية وعدم استقراره في مصل الدم. في هذه الدراسة، تم توظيف تقنية النانو لتحسين إيصال هذا الدواء عن طريق تصنيع مستحلب نانوي، حيث تم استخدام نوعين مختلفين من المبلمرات هما *Polyethylene glycol* (*PEG*) وPolycaprolactone (*PCL*), لتحسين استقرار جزيئات المستحلب النانوية وزيادة توافقها الحيوي وتقليل كرهها للماء، وبالتالي بقاءها فترة أطول في الدورة الدموية وزيادة كفاءة العلاج.

تم استخدام *PEG* و*PCL* بثلاث نسب مختلفة بما في ذلك 25:75 و50:50 و75:25، للكشف عن أنسب الخصائص للجسيمات النانوية (*NP*) لإيصال الدواء، حيث تم دراسة العينة المصنعة من $Cu(DDC)_2$ باستخدام جهاز مطيافية الأشعة تحت الحمراء *FT-IR spectroscopy* و الطيف المرئي "فوق البنفسجي" *UV-vis spectroscopy*. تم دراسة كفاءة التغليف للكبسولات المحضرة وحجم الجسيمات وإطلاق الدواء وثبات الكبسولات في المصل والسمية الخلوية للجسيمات النانوية المحضرة.